MAR 16 1990

CARRERA/



Dr. Jesus Carrera
Universidad Politechnica de Cataluna
ETSI Caminos
Jordi Girona Salgado, 31
08034 Barcelona SPAIN

Dear Jesus:

I was glad to see you again at the INTRAVAL meeting in Las Vegas last February. I hope that you can still find the time from your busy schedule to attempt problem 6 on the synthetic migration experiment. I have enclosed a complete set of information consisting of the floppy disk and the problem statement for your convenience. Hopefully, I have lined up several interested groups of people to work on the problem including Lloyd Townley, Paul Davis, a group from NRC which includes Ralph Cady, and possibly Brit Jacobson under contract from the Center for Nuclear Waste Regulatory Analysis, which is our new laboratory. I was encouraged by my own results using simple methods, and am anxious to see how some of these more powerful tools would do.

I will be performing simulated pump tests on at least two other locations to fill in some of the data-poor areas of the field. I will send them to you when they are completed so that you can factor the data into your calculations if you wish.

I will be in Madrid from March 25 to 30. I can make it up to Barcelona on Friday the 30th or Saturday the 31. Please let me know if this would be convenient. If not, I would still appreciate getting your codes by mail. You can reach me by phone at (301)-492-0408 or by BITNET via VZZ@NIHCU.

Sincerely,

/s/

Richard Codell, Senior Hydraulic Engineer
Division of High-Level Waste Management
Office of Nuclear Material Safety
and Safeguards

Enclosures:
1. Synthetic data disk
2. INTRAVAL Problem 6 description

DISTRIBUTION

| | | |
|---|---|---|
| Central Files | HLGP r/f | NMSS r/f |
| RBrowning, HLWM | BJYoungblood, HLWM | JBunting, HLEN |
| RBallard, HLGP | JLinehan, HLPD | RCodell, HLGP |
| SCoplan, HLGP | | |

| OFC : | HLGP RC | : HLGP | : HLGP | : | : | : |
|---|---|---|---|---|---|---|
| NAME: | RCodell/cj | : SCoplan | : | : | : | : |
| Date: | 3/14/90 | : 3/16/90 | : / /90 | : / /90 | : / /90 | : / /90 |

9003200332 900316
NMSS SUBJ
412 CDC

412
NHXV

4th INTRAVAL Workshop
Las Vegas, Nevada USA,
February 5-10, 1990

Synthetic Migration Experiment
INTRAVAL Problem 6

# PROGRESS REPORT ON INTERPRETATION OF SYNTHETIC DATA

by
Richard Codell, U.S. Nuclear Regulatory Commission
Washington D.C. 20555

## I INTRODUCTION

I have begun to interpret the "data" generated from the synthetic geosphere. The synthetic geosphere is a computer model patterned after the migration experiment in a single fracture plane at the Grimsel Rock Laboratory in Switzerland. The location of the boreholes is shown in Figure 1.

The synthetic data fall into the following categories:

1. steady state heads in closed boreholes.
2. steady state flows in open boreholes and tunnels.
3. steady state heads in response to opening other boreholes.
4. Transient flows from open boreholes and transient heads in observation boreholes.
5. dipole tracer tests between two sets of boreholes.

The aim of the exercise is to use the available data to adjust the coefficients of a computer model, and to then use that model to predict the outcome of tracer tests not included in the data set. The tracer is represented in the model by diffusionless, nonsorbing particles which advect with the groundwater flow. The problem identification stipulates certain conditions under which the synthetic geosphere operates, such as two-dimensional flow in the fracture plane only, no sorption and no molecular diffusion out of the plane of the fracture. This stipulated information partially compensates for information that might normally be available to investigators in the field but has no meaning in the context of a synthetic geosphere.

## II. ESTIMATION OF MODEL PARAMETERS

The interpretation of the data was developed in several stages:

### A. Transmissivities

Transient flow tests were used to calculate transmissivities (and storativities) at and between boreholes. A graphical procedure called the Jacob-Lohman method (DeMarsily, 1986) for artesian wells

was used to calculate single-well transmissivities from the flowing boreholes. There was no suitable method found for interpreting interference information from the observation boreholes, so a transient test based on numerical convolution of the Dupuit equation was used to calculate drawdown in the observation wells:

$$\Delta H = \frac{1}{4\pi T} \int_0^t \frac{Q(\tau)}{t-\tau} \exp\left(-\frac{r^2 S}{4T(t-\tau)}\right) d\tau \qquad (1)$$

where T is the transmissivity, t is the time, $\Delta H$ is the drawndown in the observation well, Q is the flowrate of the borehole, r is the radius of the observation well from the borehole, and S is the storativity.

The error between the observed and calculated drawdown was then minimized with a two-dimensional Powell conjugate directions algorithm (Press, 1986) to estimate transmissivity and storativity. Heads, transmissivities and storativities are given in Table 1.

B Effective Thickness

Dipole tracer tests were used to determine effective thickness of the fracture plane. This was done in two ways. First, I assumed uniform isotropic conditions between the dipoles, with a background velocity superimposed (see IIIb below). I then simulated the transport of particles in the potential field by numerical integration along the streamlines, with a random component of movement added to simulate mechanical dispersion. I manually chose values of effective thickness and dispersivity to minimize the error between the measured and predicted breakthrough curves for boreholes pairs 4-6 and 9-7. A value of effective thickness b = 0.01 meter and dispersivity alpha = 0.1 m were found to fit the measured breakthroughs reasonably well. The measured and predicted breakthrough curves for this procedure are shown in Figures 2 and 3 for dipole tests 4-6 and 9-7 respectively.

For the numerical solution with nonuniform transmissivities I also used a particle tracking routine with random dispersion to simulate tracer breakthrough, but velocities were calculated from the hydraulic heads, transmissivities and an assumed cubic relationship between effective thickness and transmissivity:

$$b = C_T (T)^{1/3} \qquad (2)$$

The factor $C_T$ is determined from the transmissivities and breakthrough curves measured from the four boreholes where there were dipole tracer tests. I used the numerical solution for flow between the dipole test at boreholes 4-6 to estimate a value of $C_T$ of about 0.5. The measured and simulated breakthrough curves for this procedure are shown in Figure 4. An attempt to use a similar numerical solution for breakthrough between boreholes 9-7 did not work well because the simulation predicted very low capture of the

tracer as shown in Figure 5. Breakthrough results are summarized in Table ~~X~~ 3.

## III Estimation of Tracer Migration

### A. Validation Tracer Tests

There were three validation data sets to test the model which involved the simulation of tracer released from boreholes 4, 5 and 11, with an injection flow rate of 0.05 liters per minute, and with a discharge from boreholes 6, 7, 8, and 9 of 0.1 liters per minute or the maximum outflow, whichever is less.

### B. Validation of Potential Flow Model

I used the potential flow model for uniform isotropic media as a first cut for predicting the breakthrough of the validation tracer tests. The velocity field was developed from superposition solutions based on steady state potential theory for a uniform fracture thickness (Javendel, 1984). This analysis did not make use of the information on borehole hydraulic tests. The velocities were assumed to be determined by the measured steady state flowrates from the boreholes and the tunnels given in Table 2, superimposed on a regional flowrate. The regional flow was determined from a numerical solution of the hydraulic heads calculated for a uniform medium with the boundary conditions stipulated for the large scale cross section of the Grimsel site given in the INTRAVAL Problem Description. The head field is shown in Figure 6. From this figure, I determined the regional flow rate to be 2.53E-7 $m^3/m$ with a direction of -54 degrees from horizontal. Tracer breakthrough was calculated with a particle tracking algorithm and random dispersion, using the effective thickness and dispersivity extracted from the dipole tests.

Results of this initial validation run with the simplified model are generally poor. Curves comparing predicted and measured breakthrough are shown in Figures 7 and 8 for releases from boreholes 5 and 11 respectively. In both cases, the model correctly predicted that all tracer would arrive at the experimental drift, but the breakthrough times are in poor agreement. Releases from borehole 4 were predicted to mostly arrive at the experimental drift, whereas the measured synthetic data indicate that nearly all tracer would be captured in borehole 9. Breakthrough results for the potential and numerical solutions are summarized in Table 3.

### C. Validation of Finite Difference Model

The interpretation of the transient borehole data allowed estimates of transmissivities at 18 locations. Heads were available at 8

boreholes and on the faces of the tunnels. I calculated variograms on the transmissivity and pressure (head minus elevation), which are shown in Figures 9 and 10 respectively. In both cases a linear variogram appeared to fit the data best. These variograms were then used with Kriging to estimate the values of transmissivity and head shown in Figures 11 and 12, respectively. Kriging variances were also calculated but are not shown.

The Kriged transmissivities and heads were subsequently used in the two-dimensional numerical algorithm to calculate steady state heads. Flowrates were specified for each borehole and hydraulic head was specified on the walls of the experimental drift and on the boundaries of the computational area. The calculated hydraulic head for the simulation is shown in Figure 13. The model calculates that the influx to the experimental drift would be 3.17E-5 $m^3$/sec, whereas the measured influx was 3.88E-5 $m^3$/sec.

The simulated breakthrough of tracer released at borehole 5 and arriving at the experimental drift is shown in Figure 14, along with the "measured" breakthrough from the synthetic geosphere experiment. The simulated breakthrough predicts capture of only about 53% of the released tracer, with the rest being lost at the bottom boundary. The "measured" breakthrough shows total capture at the experimental drift. Other than this discrepancy, the arrival times at the experimental drift are approximately the same.

The simulated breakthrough of tracer released at borehole 4 is shown in Figure 15 along with the "measured" breakthrough. In this case, the simulation correctly predicts that most of the capture occurs at borehole 9 (97.7% predicted, 91.6% measured), although at a somewhat slower rate.

## IV Conclusions

I have performed a preliminary interpretation of the data generated on the synthetic geosphere with limited success in predicting the breakthrough of non-sorbing tracer. The expedient analysis using potential theory was useful but did not yield accurate results because of the highly variable hydraulic properties built into the synthetic geosphere. Numerical solution of the flow field with Kriged transmissivities and heads was somewhat more successful, but the small number of samples in parts of the computational field contributed to large errors in the boundary conditions and transmissivity values from extrapolation outside of the range of the data. Repeating the analyses with a few more boreholes placed in selected spots in the field would add to the accuracy of the solution. Furthermore, I have employed only straightforward analytical tools based on the assumption of local homogeneity to analyze drawdown tests, and therefore probably have not extracted as much information from the available data as possible. I have not tried to exploit the expected correlation between measured transmissivity and head, but this might lead to more accurate

predictions. Other data that I did not use included flowrates to the tunnels other than the experimental drift, and the steady state effect on heads resulting from opening each borehole.

For the next phase of the interpretation I plan the following:

1. Determine a good location to place a few more boreholes to measure heads, transient drawdown tests and dipole tracer tests. Repeat the predictions made above with these additional data.

2. Use more powerful interpretive tools to extract more information from the data; in particular the relationship between transmissivity and head.

## V. References

De Marsily, G. , 1986 Quantitative Hydrogeology, Academic Press, Orlando,

Javandel, I, C. Doughty, and C.F. Tsang, 1984, Groundwater Transport, American Geophysical Union, Monograph 10, Washington DC, 1984

Press, H., B.Flannery, S.Teukolsky, and W.Vetterling, Numerical Recipes, Cambridge University Press, Cambridge, 1986

Table 1 - Measured Transmissivities, Storativities and Heads

| Location | x-m | y-m | T - $m^2/s$ | H - m | S | Test Type |
|---|---|---|---|---|---|---|
| BH4 | -10.3 | -6 | 3.76E-7 | 6.105 | 9.67E-7 | J-L[1] |
| BH5 | -5.8 | 3.65 | 2.34E-7 | 0.8 | 2.72E-6 | J-L |
| BH6 | -4.6 | -5.3 | 5.4E-7 | 2.95 | 2.56E-6 | J-L |
| BH7 | -6.05 | -3.5 | 1.33E-6 | 3.74 | 1.61E-8 | J-L |
| BH8 | -1.5 | -4.5 | 4.95E-7 | 0.49 | 1.76E-7 | J-L |
| BH9 | -6 | -7.5 | 2.64E-7 | 3.81 | 2.14E-6 | J-L |
| BH10 | 3 | -2.7 | 6.16E-7 | -0.31 | 2.8E-7 | J-L |
| BH11 | -15.3 | 4.0 | 1.71E-6 | 8.92 | 2.54E-4 | J-L |
| BH4-6 | -7.45 | -5.65 | 1.065E-6 | | 1.568E-6 | Int.[2] |
| BH4-7 | -8.175 | -4.75 | 1.64E-6 | | 1.54E-6 | Int. |
| BH4-9 | -8.15 | -6.75 | 5.93E-7 | | 1.36E-6 | Int. |
| BH5-8 | 2.15 | -4.075 | 3.08E-6 | | 6.21E-6 | Int. |
| BH5-10 | 4.4 | -3.175 | 7.81E-7 | | 1.23E-6 | Int. |
| BH6-7 | -5.325 | -4.4 | 1.17E-6 | | 1.03E-6 | Int. |
| BH6-8 | -3.05 | -4.9 | 1.43E-6 | | 1.18E-6 | Int. |
| BH6-9 | -5.3 | -6.4 | 5.25E-7 | | 8.84E-7 | Int. |
| BH7-4 | -8.175 | -4.75 | 1.52E-6 | | 1.24E-6 | Int. |
| BH7-6 | -5.325 | -4.4 | 1.17E-6 | | 9.74E-7 | Int. |
| BH7-8 | -3.775 | -4 | 3.39E-6 | | 1.67E-6 | Int. |
| BH7-9 | -6.025 | -5.5 | 1.08E-6 | | 1.04E-6 | Int. |
| BH8-6 | -3.05 | -4.9 | 1.34E-6 | | 1.14E-6 | Int. |
| BH8-7 | -3.775 | -4 | 3.01E-6 | | 1.93E-6 | Int. |
| BH8-9 | -3.75 | -6 | 1.11E-6 | | 1.78E-6 | Int. |
| BH9-4 | -8.15 | -6.75 | 5.86E-7 | | 1.40E-6 | Int. |
| BH9-6 | -5.3 | -6.4 | 5.13E-7 | | 9.30E-7 | Int. |
| BH9-7 | -6.025 | -5.5 | 1.03E-6 | | 1.22E-6 | Int. |
| BH10-5 | 4.4 | -3.175 | 7.95E-7 | | 1.22E-6 | Int. |
| BH10-8 | 0.75 | -3.6 | 5.78E-6 | | 3.13E-6 | Int. |

[1]Jacob-Lohman single well test based on flow rates

[2]Interference test. First borehole is flowing, second is observation well. See text for explanation of procedure.

Table 2 - Flows for Potential Flow Analysis

| Location | x-m | y-m | R-m | Q - $m^3$/sec [3] |
|---|---|---|---|---|
| Tunnel 5 | -40 | 0 | 1.75 | -4.055E-5 |
| Tunnel 6 | 0 | 0 | 1.75 | -3.88E-5 |
| Tunnel 7 | 33 | 3.75 | 2.5 | -4.79E-6 |
| Tunnel 8 | 53 | 2.6 | 1.6 | -3.7E-6 |
| Borehole 4 | -10.3 | -6 | 0.043 | 8.33E-7 |
| Borehole 5 | 5.8 | -3.65 | 0.043 | 8.33E-7 |
| Borehole 11 | -15.3 | 4 | 0.043 | 8.33E-7 |
| Borehole 6 | -4.6 | -5.3 | 0.043 | -1.64E-6 |
| Borehole 7 | -6.05 | -3.5 | 0.043 | -1.67E-6 |
| Borehole 8 | -1.5 | -4.5 | 0.043 | -1.86E-7 |
| Borehole 9 | -6 | -7.5 | 0.043 | -1.32E-6 |

Background Flowrate = 2.53E-7 $m^3$/m, direction = -54 degrees

Table 3 - Summary of Breakthrough Capture Fractions

| Case | Measured Data | Simulated potential | Simulated Numerical |
|---|---|---|---|
| Dipole 4-6 | | | |
| at BH6 | 100% | 90.6% | 91.9% |
| Dipole 9-7 | | | |
| at BH7 | 47.5% | 42.8% | 11.4% |
| at drift | 52.5% | 57.2% | |
| release at BH4 | | | |
| at drift | 2.6% | 67.8% | |
| at BH6 | 5.8% | 20.2% | |
| at BH7 | 0 | 12% | |
| at BH9 | 91.6% | 0 | 97.7% |
| Release at BH5 | | | |
| at Drift | 100% | 100% | 54.2% |
| Release at BH11 | 100% | 100% | |

[3] Flowrate out of boreholes is limited to 1.67E-6$m^3$/sec or normal outflow, whichever is less.

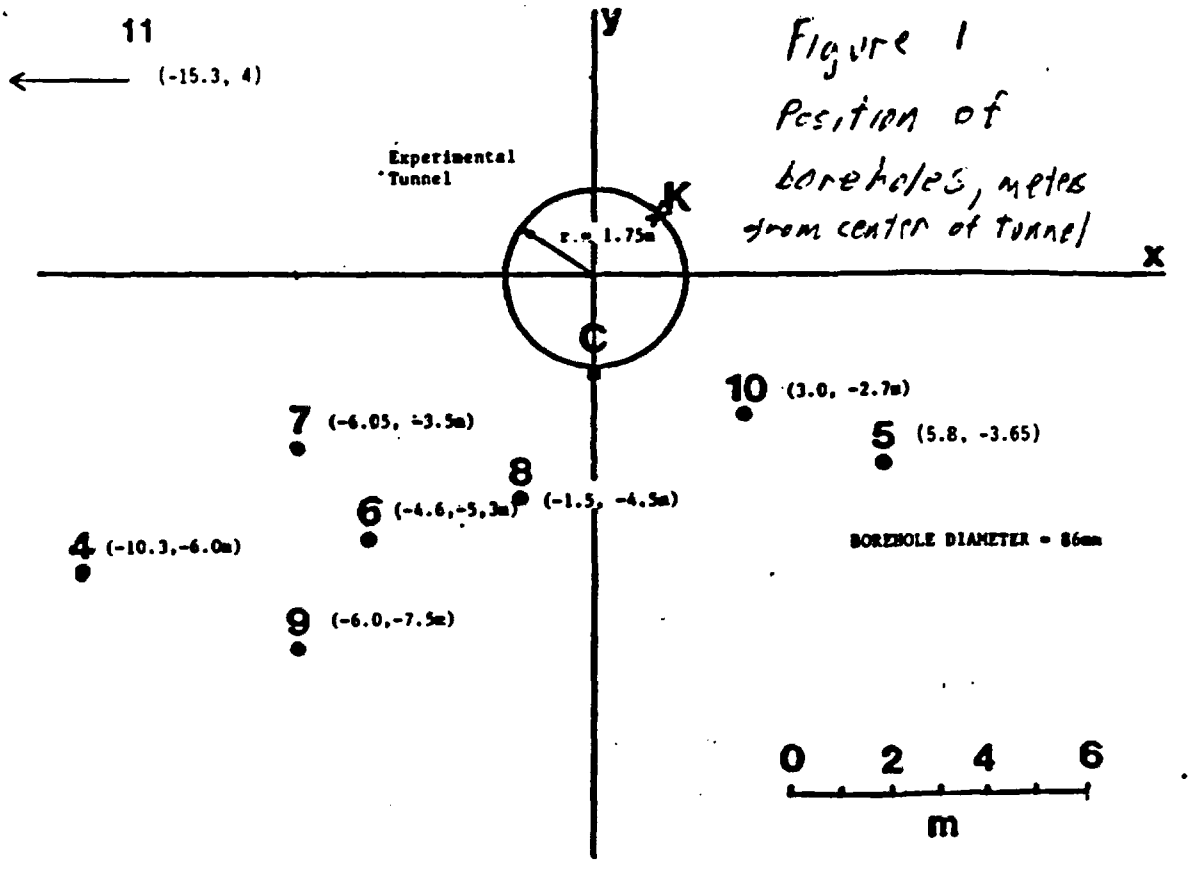


Figure 1
Position of boreholes, meters from center of tunnel

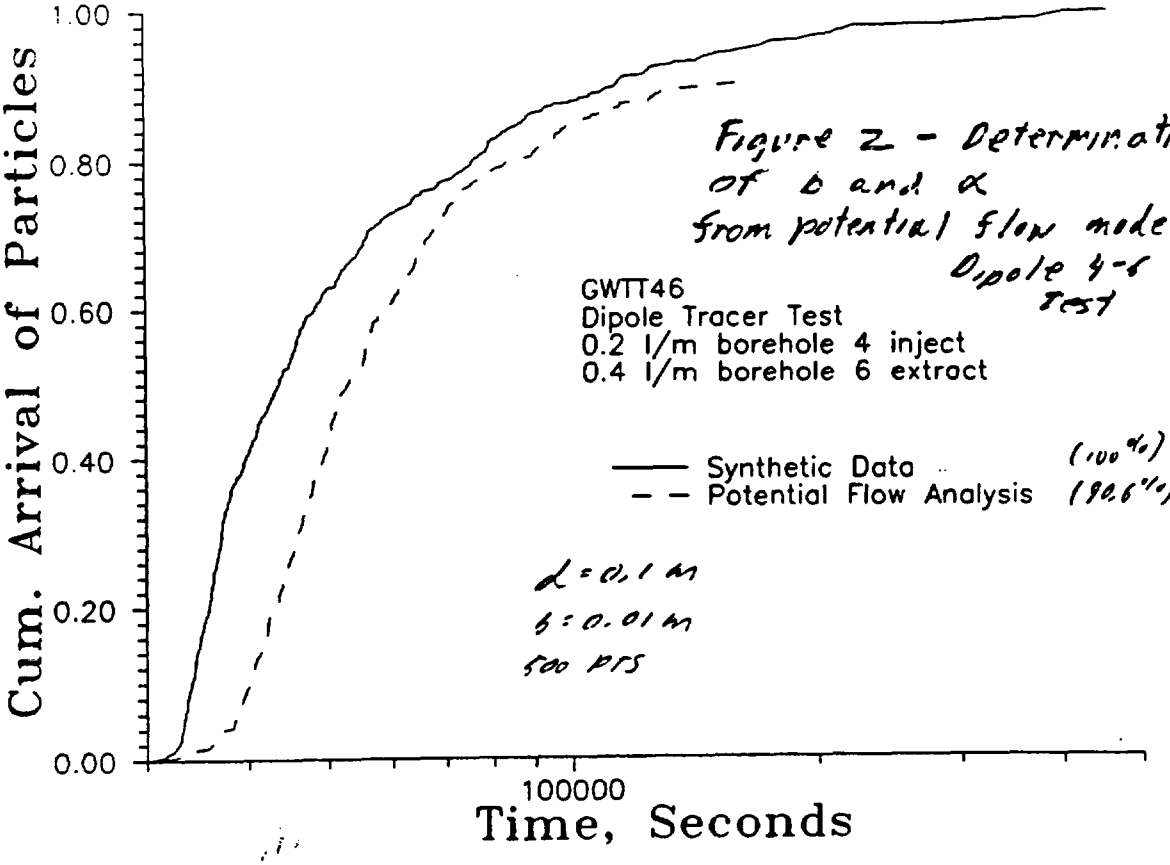


Figure 2 - Determination of b and α from potential flow model Dipole 4-6 Test

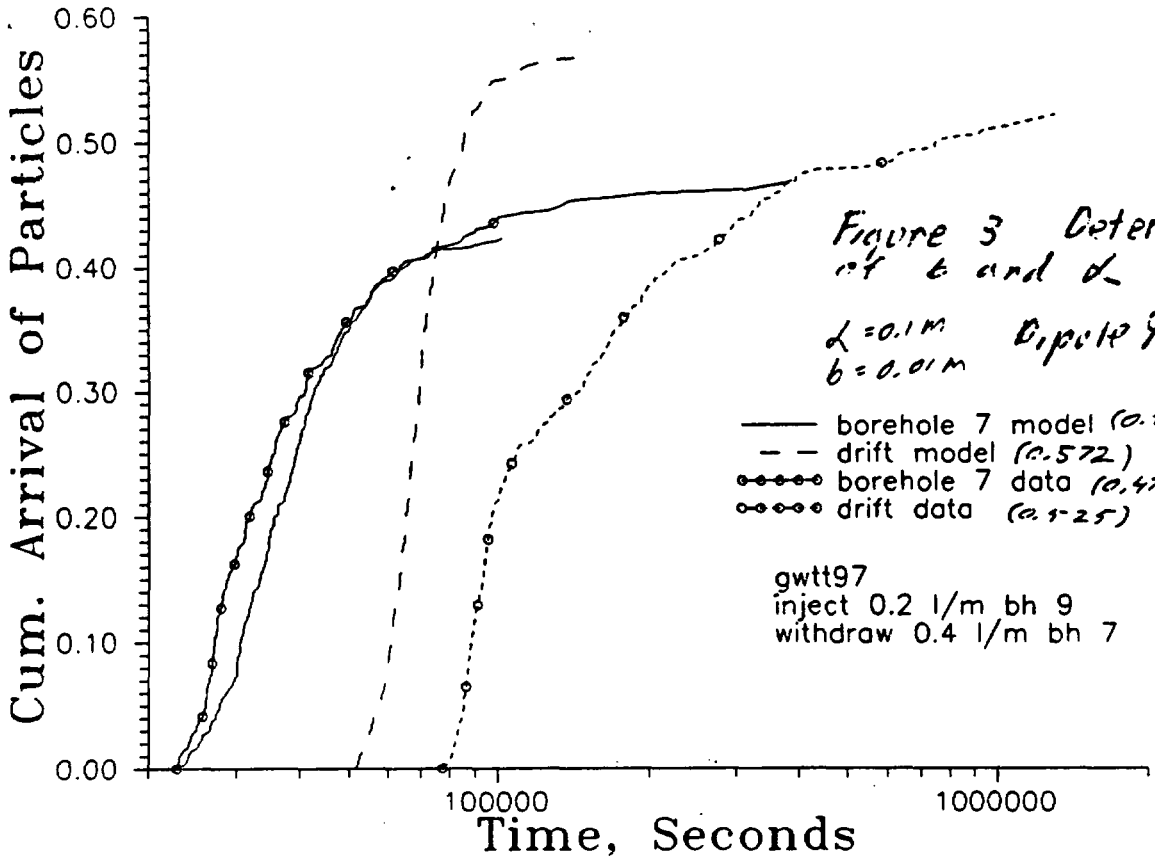


Figure 3 Determination of b and α

α = 0.1 m
b = 0.01 m
Dipole 9-7

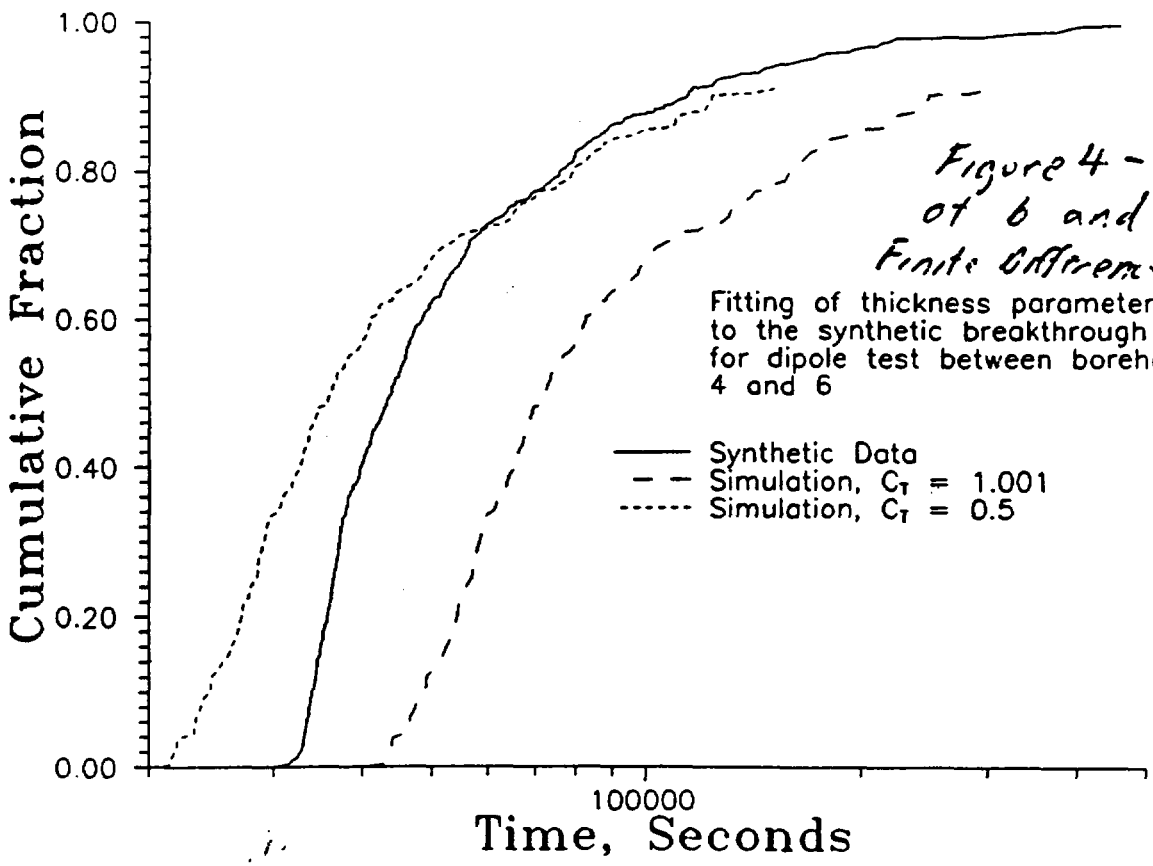


Figure 4 - Determination of b and α
Finite difference model

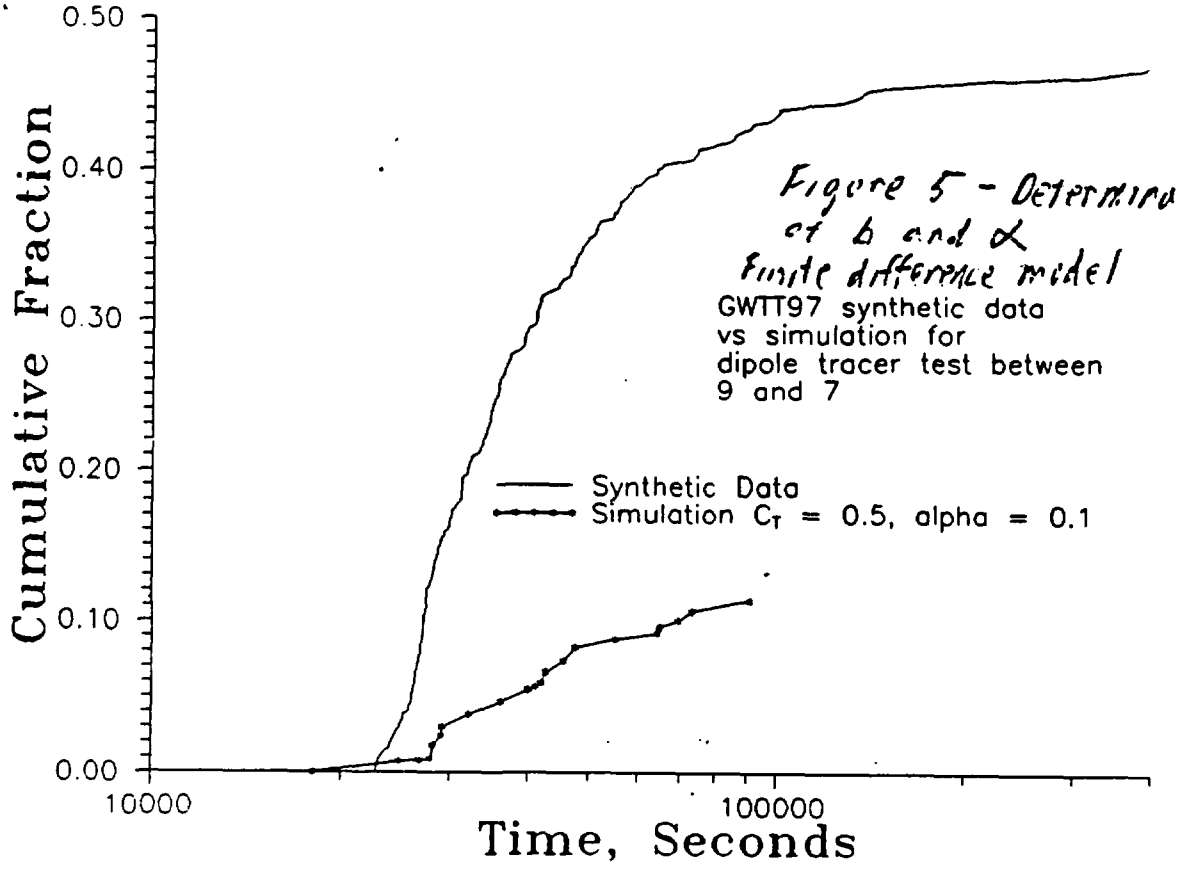


Figure 5 - Determination of b and α
Finite difference model
GWTT97 synthetic data vs simulation for dipole tracer test between 9 and 7

Figure 6 - Mountain Cross Section

Direction of regional flow

Hydraulic heads, no tunnels, constant T

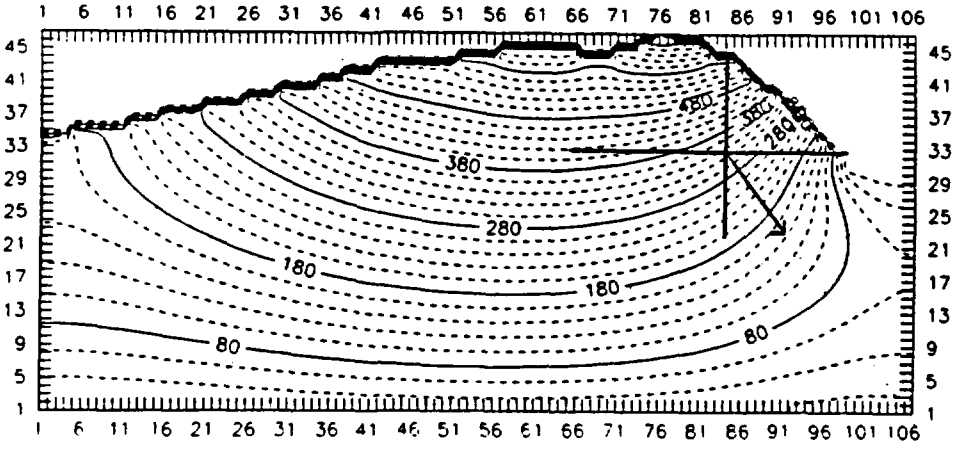

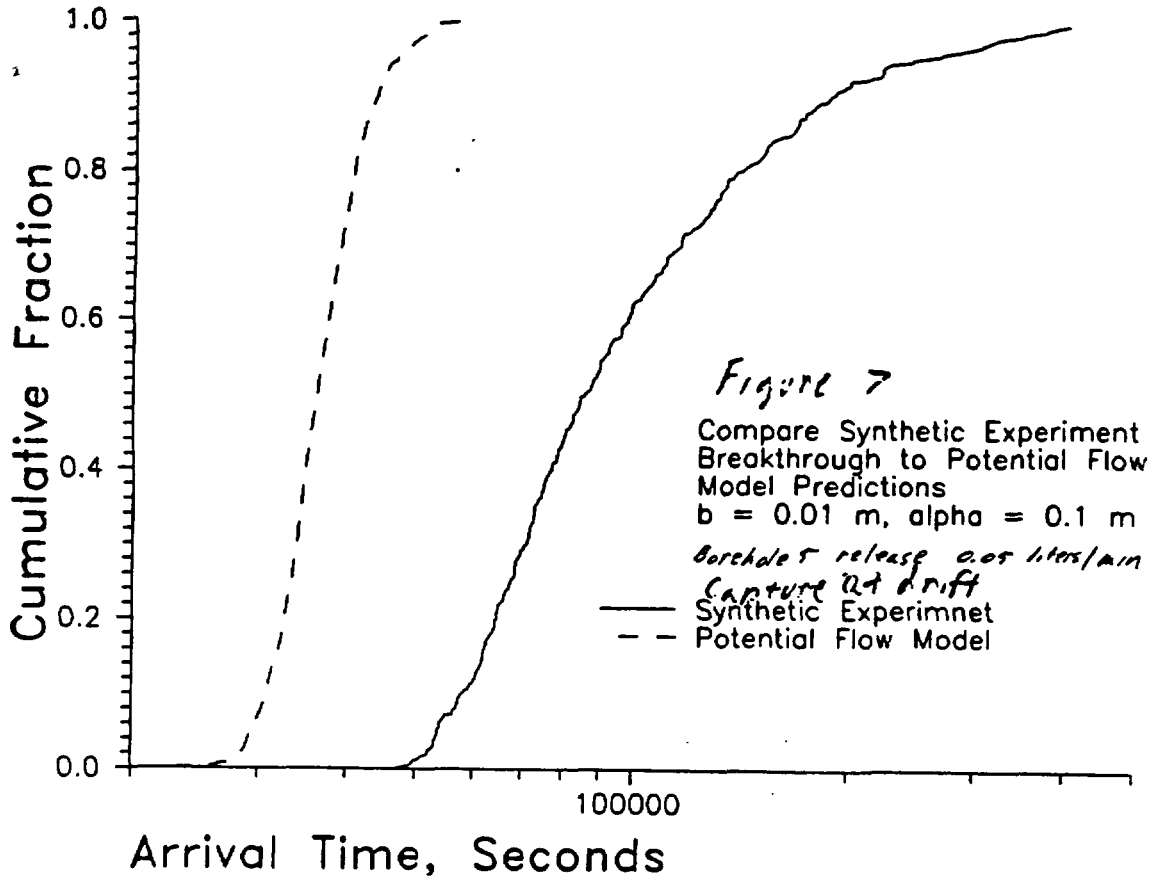


Figure 7

Compare Synthetic Experiment Breakthrough to Potential Flow Model Predictions
b = 0.01 m, alpha = 0.1 m
Borehole 5 release 0.05 liters/min
Capture at drift

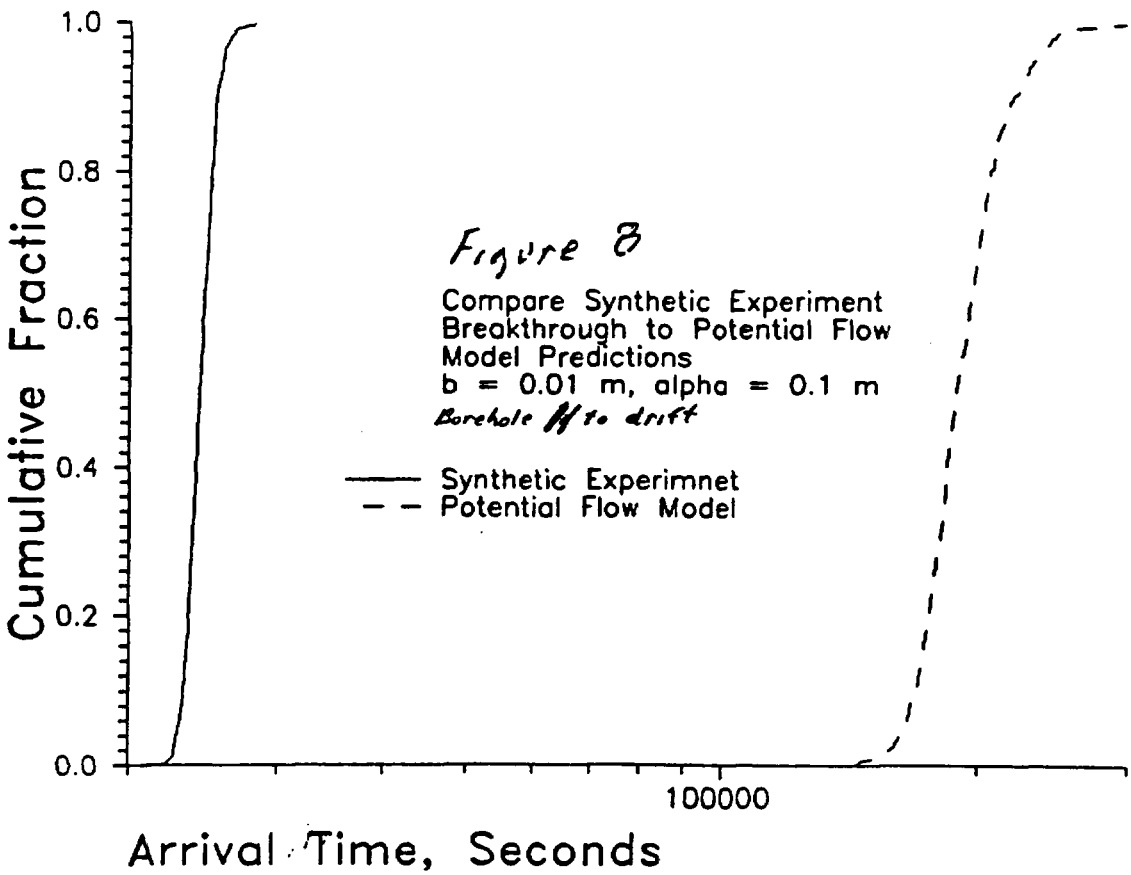


Figure 8

Compare Synthetic Experiment Breakthrough to Potential Flow Model Predictions
b = 0.01 m, alpha = 0.1 m
Borehole 11 to drift

Figure 9

Variogram for log T

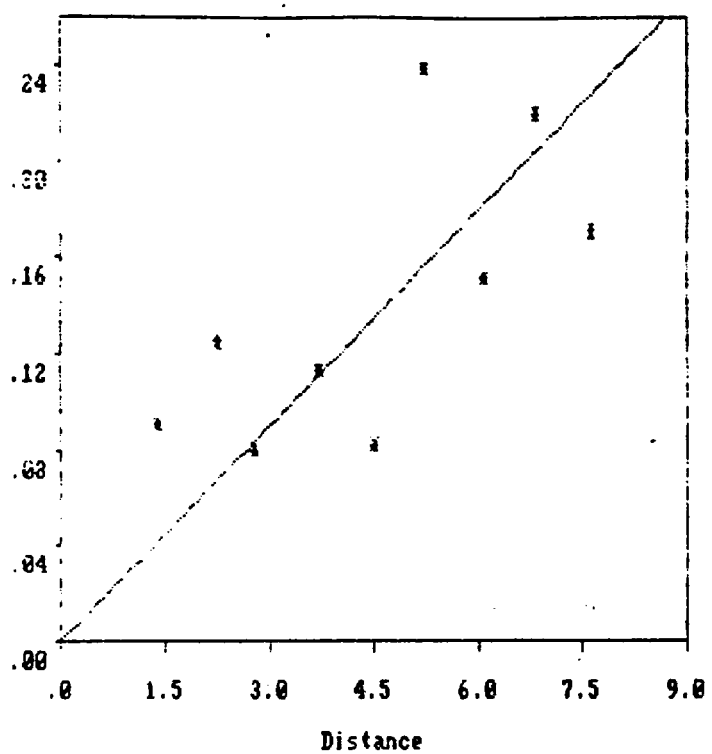


Parameters

File :trans.pcf

Pairs : 235

Direct.: .000

Tol. : 90.000

MaxBand: n/a

log T Limits

Minimum: -6.631

Maximum: -5.238

Mean : -6.087

Var. : .12791

Figure 10

Variogram for HEAD (Pressures)

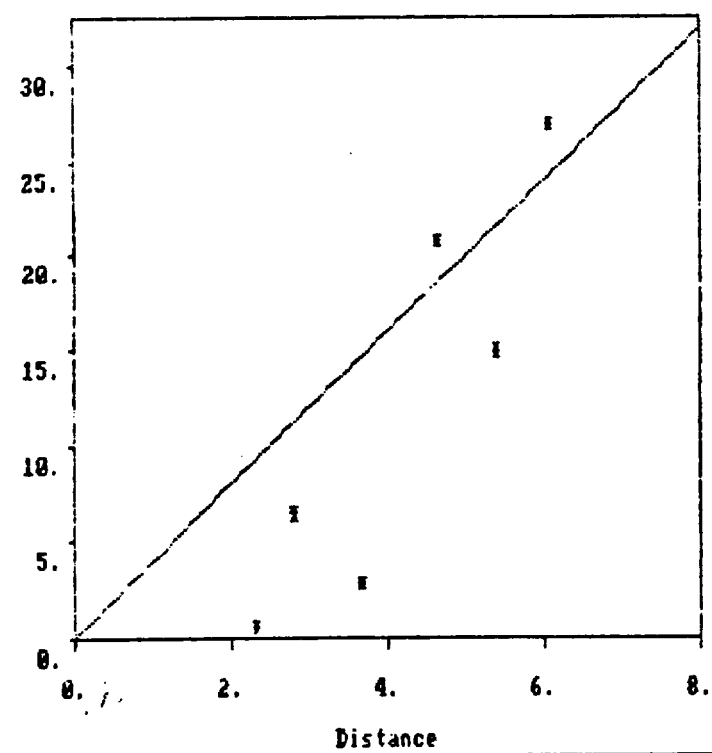


Parameters

File :head.pcf

Pairs : 31

Direct.: .000

Tol. : 90.000

MaxBand: n/a

HEAD Limits

Minimum: .000

Maximum: 12.185

Mean : 5.138

Var. : 21.698

Figure 11

KRIGED LOG T FROM SYNTHETIC EXPERIMENT $m^2/sec$

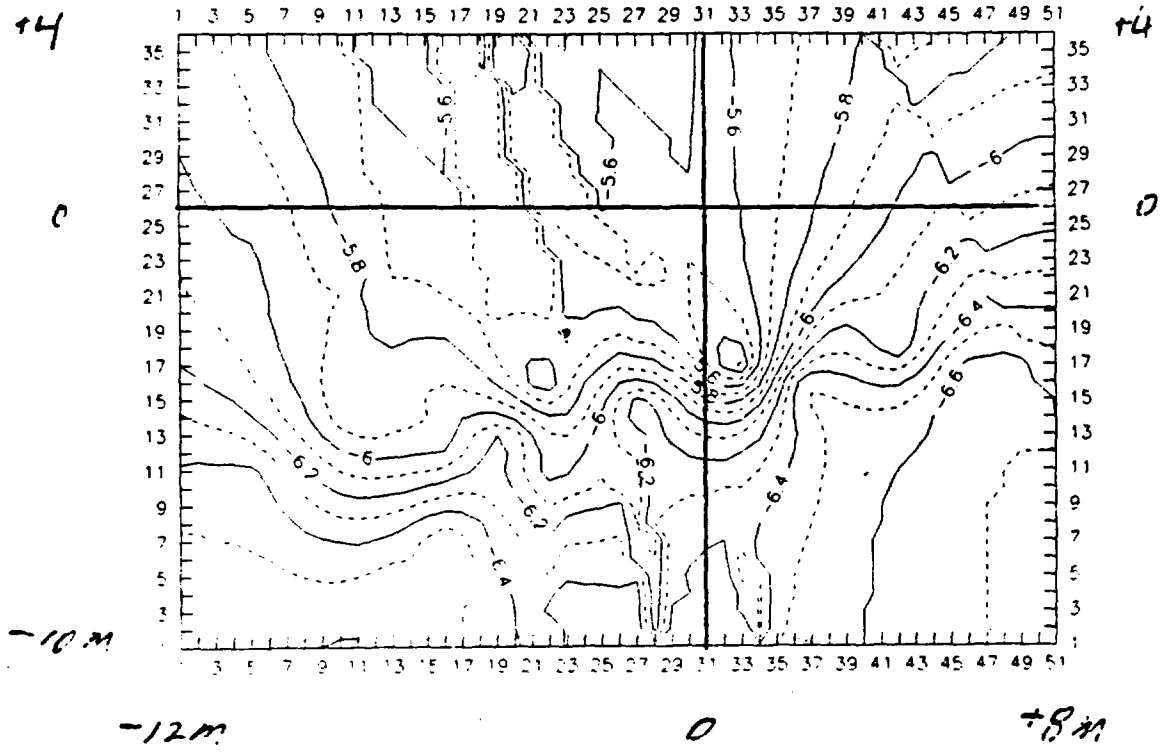


Figure 12

INITIAL HEADS FROM KRIGING SYNTHETIC EXP meters

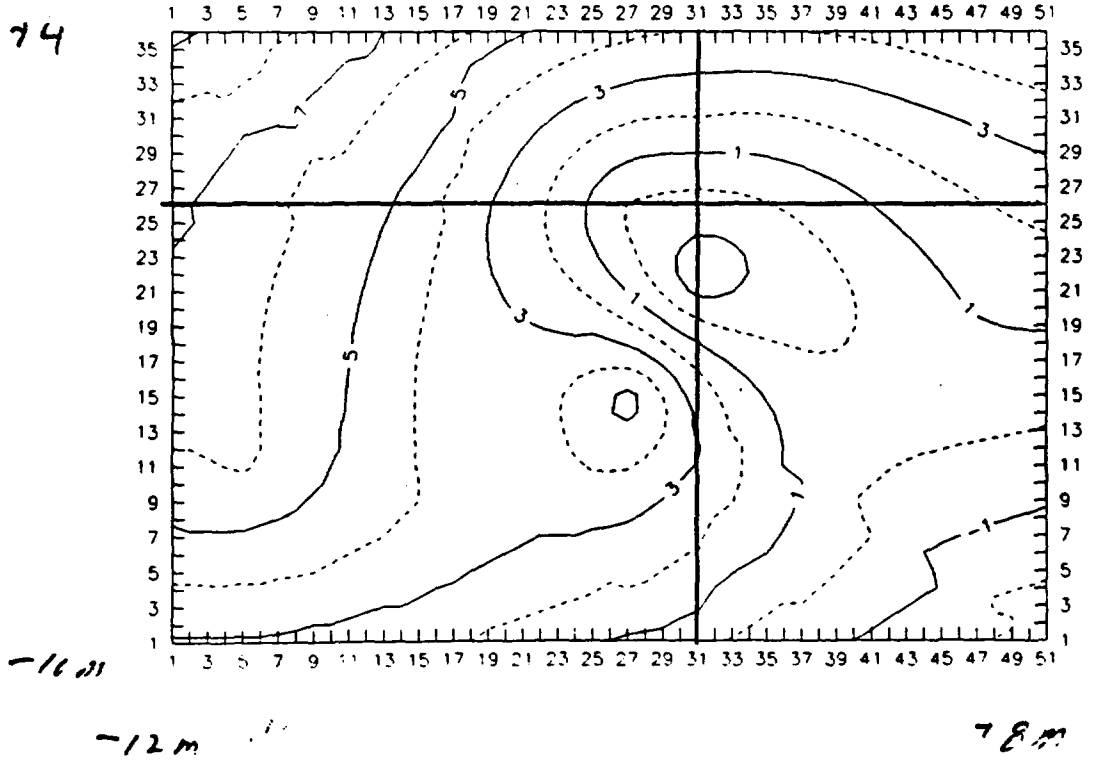

Figure 13 - Calculated

HEADS FOR TRANSPORT PROBLEM

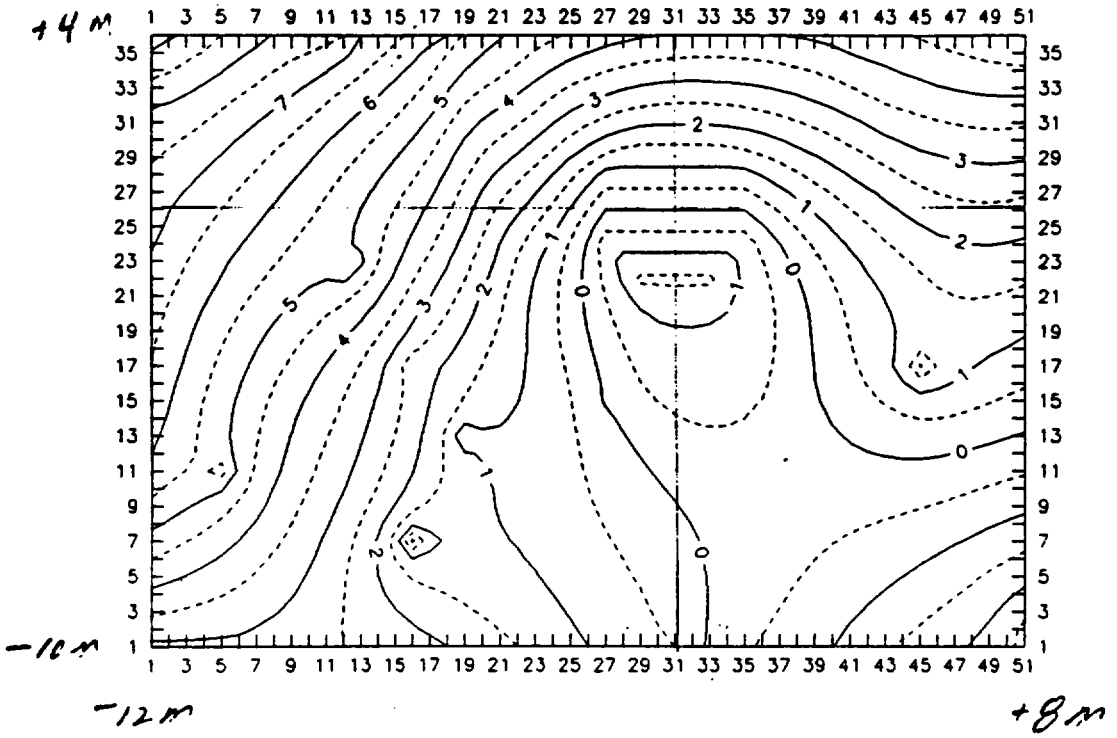


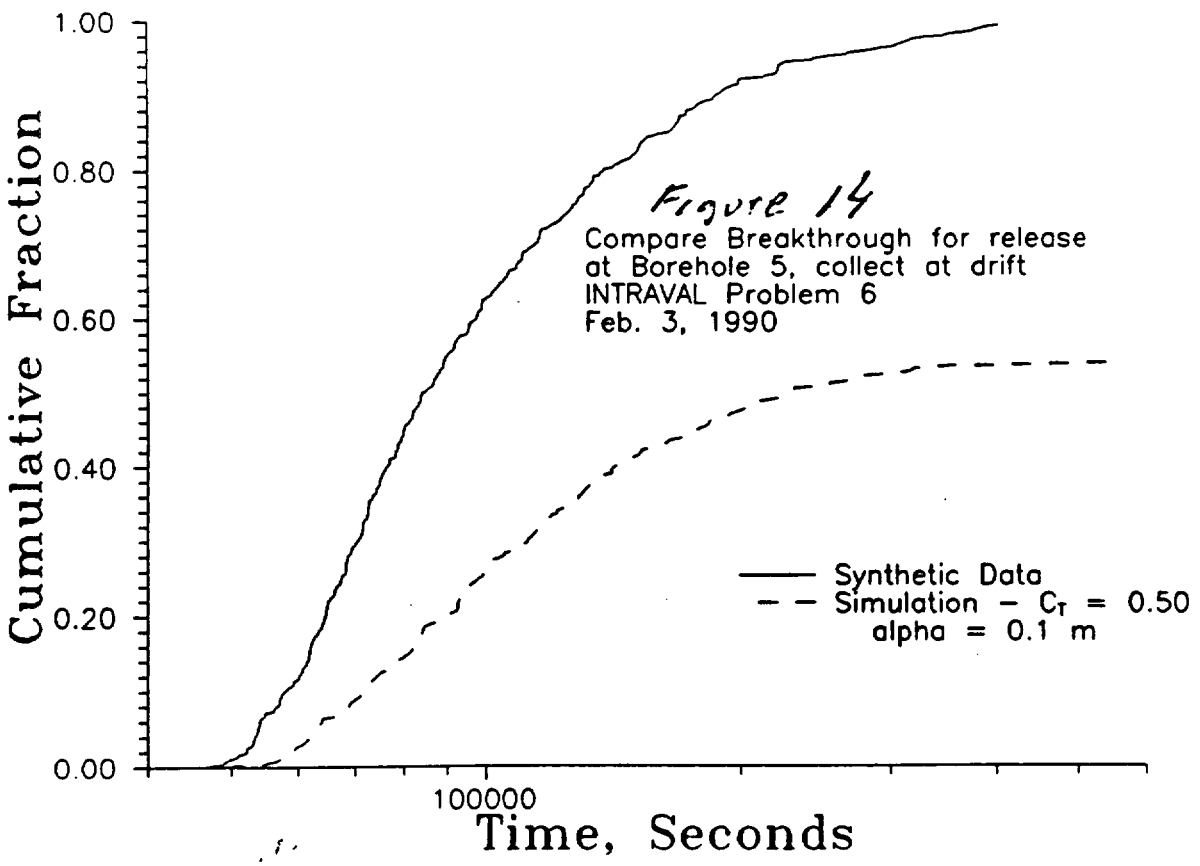


Figure 14

Compare Breakthrough for release at Borehole 5, collect at drift
INTRAVAL Problem 6
Feb. 3, 1990

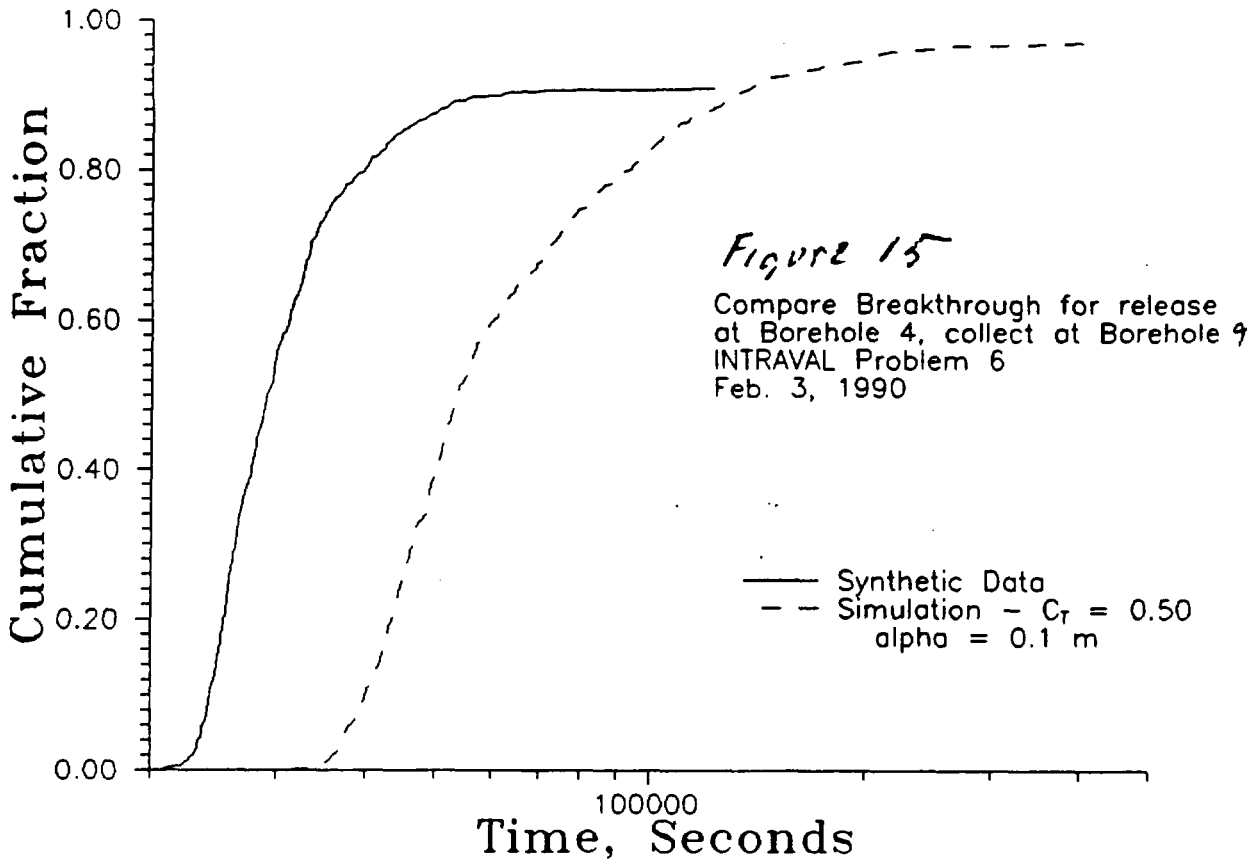


Figure 15

Compare Breakthrough for release at Borehole 4, collect at Borehole 9
INTRAVAL Problem 6
Feb. 3, 1990

# INTRAVAL Test Case 6

## Synthetic Migration Experiment

U.S. Nuclear Regulatory Commission
Battelle Pacific Northwest Laboratories
NAGRA

May 1989

For the Third INTRAVAL Workshop
Helsinki Finland, June 12-16, 1989

# INTRAVAL

## Synthetic Migration Experiment

### Phase I - Non-Diffusing Inert Tracer

## I. INTRODUCTION

This document identifies INTRAVAL Case 6, which deals with the modeling of hydraulic and tracer migration tests at a synthetic site patterned after the tracer migration experiment at the Grimsel Rock Laboratory in Switzerland.

A. Pilot Group Identification - Joint U.S. Nuclear Regulatory Commission, Battelle Pacific Northwest Laboratories, and NAGRA. The pilot team consists of the following individuals:
   1. Richard Codell, USNRC
   2. Charles Cole, Pacific Northwest Laboratories
   3. Stratis Vomvoris, NAGRA.

B. Experimental Location - This site is synthetic, and therefore exists only as concepts in digital computer programs. Geologic and hydrologic boundaries, and the mean, variance and spatial correlation scales of the model parameters are conditioned with real-world data from the Grimsel Rock Laboratory in Switzerland. The synthetic site is intended to resemble an instrumented single fracture plane in a mountainous, granitic geosphere, similar to such a fracture plane at Grimsel. We emphasize that the conditioning process is not meant to make the synthetic geosphere represent the real site. The purpose of the conditioning is to set the problem parameters and scales so that the synthetic site is plausible.

C. Objectives - The object of this synthetic experiment is to help improve our understanding of the "identifiability problem" which plays an important role in the validation process. Identifiability problems arise because of the variability (both spatial and temporal) in geometry, parameters, boundary conditions, and competing processes (e.g., in the sense that they produce similar effects in terms of observable transport results). In turn, the variability problem leads to the important and related issues of measurement scale, sampling density and location, interpretation and interpolation. These problems can be examined to some degree with synthetic experiments. We have developed a highly detailed, realistic but synthetic geosphere whose geometry, processes and parameter ranges have been conditioned in a broad sense with both quantitative and qualitative data from a real-world site, the Grimsel Rock Laboratory. We have conducted a limited number of experiments, much like those already performed and proposed for the Grimsel site, through numerical simulations with our synthetic geosphere. We provide the project teams that participate in this experiment with hard (quantitative) data in the form of simulated measurements from the numerical experiments along with soft

(qualitative) information of the type used to design the numerical experiments and condition the data sets used in the synthetic geosphere. We have attempted to supply these descriptions and the data in a form and in quantities equivalent to that which would be available at the real site.

Project teams participating in this test case will be expected to treat it like any other (real) experiment. From the qualitative and quantitative descriptions of the site, the measurements, and the various experiments, the project teams would be expected to calibrate their models and make predictions for other experiments made on the same configuration. The modelers will assess the uncertainty in their predictions based on the state of model calibration achieved, and make recommendations for ways to improve the identifiability process (e.g., additional measurements, different experiments, different tracers). We hope that project teams will use a variety of geostatistical, inverse, stochastic, and deterministic methods for interpreting the data, modeling, calibrating, assessing uncertainty, and making predictions. We can develop a better understanding of different strategies to interpret and model the synthetic geosphere by comparing the predicted performance measures to the "true" measures.

D. Theories Tested - The synthetic migration experiment will partially test the ability of existing groundwater flow and transport modeling strategies to interpret and characterize transport of tracer, including an assessment of the uncertainty in the interpretation and the ability to predict based on this uncertain interpretation, through a large fracture zone on the basis of a sparse network of borehole hydraulic tests, dipole tracer tests and other observations. This synthetic experiment would provide a better understanding of various geostatistical, inverse, stochastic, and deterministic methods (i.e., groundwater modeling strategies) for interpreting the data and making predictions of the performance complete with estimates of the uncertainty in spatially variable systems with competing processes.

E. Validation Aspects - The data on the complete synthetic geospheres will be used to calculate a "true" measure of performance in great detail; e.g., the breakthrough distribution of tracer at a particular boundary. Various strategies should be tried to calculate independently the performance measure based on sparse data as they would be collected from indirect tests of the synthetic geosphere.

F. Background information - Synthetic migration experiments can fulfill an important role in INTRAVAL. Figure 1 is a schematic representation of where various experiments fit into "validation" efforts for INTRAVAL. Laboratory experiments are tightly controlled, and usually allow ample data collection, but their complexity is low. Field scale experiments are more complex, but allow a less detailed program of field exploration. Most complex of all are the full size experiments on a repository scale.

At this scale, all complexities are present, but the measurability is severely limited, and we often have only a poor picture of the phenomena of importance. Synthetic experiments can approach the complexity of field and repository scale experiments, and allow a high degree of measurability.

The idea of using a computer-generated reality on which to conduct experiments has been contemplated for several decades. The advent of inexpensive, fast computers with large memories has made the idea feasible. The idea dates at least from von Neumann, who envisioned the use of computers to generate solutions to nonlinear fluid dynamic problems. Von Neumann observed that scientists conducted difficult and expensive experiments to investigate physical behavior even when the underlying principles and governing equations were known: "The purpose of the experiments is not to verify a proposed theory but to replace a computation from an unquestioned theory by direct measurements....Thus wind tunnels are used at present, at least in large part, as computing devices of the so-called analogy type to integrate the nonlinear partial differential equations of fluid dynamics" (Winkler, 1987).

The present use of synthetic experiments is not exactly as von Neumann envisioned; e.g., the theory is not unquestioned, and unlike air in a wind tunnel, the geosphere is non-homogeneous. The analogy to using a computer for the purpose of testing a methodology instead of a real, expensive and often inadequate experimental site remains however.

There are several advantages that synthetic experiments have over real-world experiments: (1) There is no final information uncertainty when interpreting and comparing the results of conceptually different performance assessment codes; and (2) the experiment is non-destructive, allowing the exploration of different testing procedures on the same piece of computerized geosphere (Hufschmied, 1986). In addition, synthetic experiments can produce results that would be infeasible with real sites; e.g., natural gradient tracer experiments that would take hundreds or thousands of years. However, synthetic experiments can't actually determine the correct mathematical formulation for the laws that are operative in nature; only carefully controlled, real experiments can do this. Consequently, it is important for us to describe the models used in generating the experimental results in some detail so that the modelers choosing to participate in this problem are not distracted from the primary purpose of the exercise by arguments over the correct natural laws that apply in the synthetic reality. We will describe the laws governing the synthetic universe a priori, and recommend (but do not insist) that project teams modeling this synthetic experiment consider the described processes and mechanisms in any of their modeling and interpretation efforts. Our selection of certain laws for our synthetic universe is not meant as an endorsement of a particular mathematical formulation for a process, but simply allows the issue of mathematical formulation of the process laws to be excluded from the identifiability issues being studied through the use of synthetic experiments. The investigators may choose to

consider only the laws that apply to the synthetic universe. Alternatively, they may choose to use more general or different laws to interpret the data, especially if they feel that some of the mechanisms are unidentifiable with the available information. The specific nature of these laws is given below:

Laws of Nature that Apply to the Synthetic Geosphere - Our ability to construct a realistic synthetic geosphere is limited by the understanding of physical phenomena in the real world and the degree that we can discretize space so it can be represented and solved in a reasonable way on a digital computer. In order to make this a tractable exercise, the synthetic geosphere is restricted to a subset of a complete reality. The synthetic experiments are not intended to determine which laws are operative in nature. As a result it is important to define the laws that have been assumed to describe the various mechanisms in our synthetic reality. Wherever possible, the laws of nature for the synthetic geosphere are similar to laws that govern the processes in the real world.

These assumptions, processes, and mathematical formulations are:

(1) The entire modeled domain is two dimensional, in that flow is considered to take place in a single fracture zone.

(2) Advective flow in the fracture follows Darcy's Law (Eq. 1).

$$V_f = k_f \frac{\rho}{\mu} \text{ grad } h_f \qquad (1)$$

where:

$V_f$ = Darcy velocity, [L/t]
$k_f$ = permeability, [$L^2$]
$\rho$ = density, [$M/L^3$]
g = gravitational constant, [$L/t^2$]
$\mu$ = viscosity, [M/L/t]
$h_f$ = hydraulic head or potential, [L]
grad = gradient operator

The mathematical equations that govern the calculation of flow in the fracture zone are:

$$\frac{\partial}{\partial x}\left(T_{xf}\frac{\partial h_f}{\partial x}\right) + \frac{\partial}{\partial y}\left(T_{yf}\frac{\partial h_f}{\partial y}\right) + q_f = S_f\frac{\partial h_f}{\partial t} \qquad (2)$$

where:

$h_f$ = potential in the fracture at (x,y) [L]
$T_{xf}$ = transmissivity in x direction at (x,y) [$L^2/t$]
$T_{yf}$ = transmissivity in y direction at (x,y) [$L^2/t$]

$q_f$ = flow source term at (x,y) $[L^3/t]$
$S_f$ = storage coefficient $[L^0]$

The pore velocity is the velocity at which the inert, non-diffusing tracer particles will move. It is defined:

$$U_x = -\frac{T_{xf}}{\theta}\frac{\partial h_f}{\partial x} \qquad (3)$$

Similarly:

$$U_y = -\frac{T_{yf}}{\theta}\frac{\partial h_f}{\partial y} \qquad (4)$$

where $\theta$ is the effective thickness of the fracture zone. Transport is assumed to be dominated by flow in open spaces rather than through porous media, and therefore the effective thickness is proportional to the cube root of the local transmissivity. One cannot assume, however, that flow occurs in a single smooth, parallel fracture, so it would be inappropriate to estimate effective thickness directly from transmissivity.

(3) The synthetic universe is isothermal at 25 °C.

(4) Fluid properties are considered to be constant. Density of the water, $\rho$, with and without tracers is constant at 1000 $kg/m^3$.

(5) In Phase I of this study, the tracer moves strictly in the fracture plane. It does not diffuse into the rock, nor is it retarded by sorption. Simulation of sorbing tracer and matrix diffusion will be explored in Phase II.

(6) Tunnels and drifts are at atmospheric pressure, so that the hydraulic potential at this boundary is equal to the elevation. The open boreholes are connected to tubes whose outlets are at the center of the experimental drift. The head in open boreholes is therefore zero.

(7) The hydraulic potential of the land surface is equal to the elevation relative to the center of the experimental drift.

In modeling this synthetic experiment, the investigators need only consider the listed mechanisms if they so desire. It is important to reiterate that these are not the only mechanisms that can and do occur in nature, nor that these are the only or most appropriate mathematical descriptions for the proposed processes. Only properly designed, well controlled, real experiments can determine which kind of processes occur and which mathematical description is the most appropriate.

## II. EXPERIMENTAL DESIGN

A. Overview - The synthetic migration experiment for Phase I will be performed in the following steps:

1. Generate a highly detailed field of synthetic hydraulic and transport properties;

2. Generate a steady state field of hydraulic potentials (heads) by imposing boundary conditions and solving the necessary differential equations in a very fine grid. The steady state models are used to simulate the transport of tracer either introduced passively or under pressure in a dipole test. These models are also used to calculate the steady state flows to or from boreholes and tunnels.

3. Perform a limited number of simulated tests on the synthetic data base with a transient hydraulic model to estimate the hydraulic properties. Only data provided to the modeler from the indirect sampling of the synthetic geosphere may be used, not the synthetic data itself.

4. Calibrate the performance model with the available hydraulic and transport data.

5. Compute the performance measure (the breakthrough of tracer at the boreholes and drift) and the confidence in the result.

6. Recommend additional data to be collected and repeat steps 4 and 5, until satisfied with result.

7. At the conclusion of the calibration and prediction steps, compare the results of the prediction to the "true" results calculated and supplied by the pilot team using the complete synthetic geosphere.

Transmissivity for the synthetic migration experiment is generated with a fractal surface generator (Jeffery, 1987), adjusted to give values of mean, variance and spatial scaling similar to the observed data at the Grimsel site. An advantage of using the fractal landscape as an analog to transmissivity is that the data field contain multiple scales of spatial correlation, and is not restricted to stationary random processes. Distributions of properties in sedimentary environments have been characterized as "fractal", exhibiting multiple scales of correlation (Hewitt, 1986). Many properties of geologic systems are also known to have multiple scales of correlation. There are essentially three choices for treating the variability of the transmissivity; uniform throughout the domain, spatially correlated with one scale of correlation or spatially correlated with multiple levels of correlation. Of the three choices, the last is most appealing.

Effective thickness was calculated from the transmissivity information using a cubic law, adjusted to give breakthrough results in the synthetic experiment similar to those actually observed at the Grimsel site for inert tracers (Hadermann, 1988).

B. Parameters measured -

The models have been run to produce the following (simulated) hydraulic and tracer data:

1. Steady state hydraulic head at closed boreholes.
2. Transient and steady state outflow to or from open boreholes and tunnels.
3. Response to transient pressure tests in all boreholes resulting from a pressure stress in one borehole.
4. Dipole tracer tests between two pairs of boreholes.
5. Response in tunnels to borehole tests (e.g., increased or diminished flow or appearance of tracer)

Hydraulic tests are available from 8 simulated boreholes and the 4 tunnels that penetrate the fracture plane. Requests will be honored from participants to simulate tests in a limited number of additional boreholes to refine their models. Phase I is restricted to the hydraulic measurements and conservative, non-diffusing tracer tests. Future developments of this problem set will consider tracer experiments with the effects of diffusion and sorption.

C. Spatial and Temporal Scales - The simulated experiment will be patterned after a single fracture plane at the Grimsel Rock Laboratory, covering a lateral distance of a few tens of meters. Simulated experimental measurements will cover a few tens of meters, and time scales of seconds to weeks.

D. Experimental setup - The experimental design for the rock laboratory is illustrated in Figs. 2, 3 and 4. Figure 2 shows the site as it is positioned in the mountainside on a scale of kilometers. Two water bodies bound the site on either side of the mountain. The rock laboratory is shown positioned within Figure 2. The plane to be studied is an essentially vertical two dimensional fracture. At this scale the tunnels and boreholes are not individually discernible, but their effect on the potential field must be taken into account.

Figure 3 illustrates the migration fracture on a scale of several hundred meters. The individual tunnels can be seen on this scale. It is assumed that the tunnels are open to the atmosphere, and therefore the potential at their surfaces is equal to their elevation.

Figure 4 shows the migration fracture on a scale of tens of meters. The location of the boreholes in relation to the experimental shaft are given on this scale. Pressures and transmissivity values from single and multiple hole tests are provided for boreholes at the locations shown in this figure.

There is a four step modeling procedure for generating the synthetic geosphere:

1. The first step is to calculate the hydraulic head on the scale of the distance between the water bodies, about 5000 m. This is accomplished with a finite difference computer program using a 107 x 47 uniform grid with spacing of 45.5 m and the boundary conditions shown in Figure 2. The effect of the tunnels is taken into account by sink terms in which the flow rate has been estimated from analytical formulas. The transmissivity is assumed to be uniform throughout the grid at this scale. Boundary conditions for this model are given in Fig. 2. The hydraulic head is considered to be equal to the land or water surface elevation along the top boundaries and no-flow on the other three boundaries. The purpose of the solution is to specify boundary conditions for the next finer resolution solution.

2. The second model deals with the intermediate scale problem shown in Fig.3. The domain is 182 x 182 m, and is discretized into a regular finite difference grid of dimensions 513 x 513 grid cells. The transmissivity field is taken from a 4096 x 4096 fractal data set by arithmetic averaging. The topographic data are conditioned to approximately agree with the mean, variance and spatial scales for transmissivities measured at the Grimsel site. Boundary conditions of hydraulic head on the boundary of the domain are take from the coarse scale model. The hydraulic heads of the tunnels are specified to be equal to the elevation. The results of this calculation are used to set the boundary conditions for the finest scale model, and to estimate flows in some of the tunnels. The heads are solved in a 5-level multigrid finite difference program.

3. The finest scale model is represented by a 29.9 x 22.75 m area discretized into a 673 x 513 grid. Boreholes are modeled separately in a radial coordinate system, with a one cm. resolution, and matched to the rectangular grid. Each borehole is 8.6 cm in diameter. A fixed head is specified at the borehole radius in the radial system. Boundary conditions on the edges of the rectangular domain are specified by the output of the intermediate scale model. The finest level solution is used to simulate the dipole test, and to calculate the steady state inflows to the experimental tunnel and boreholes. It also supplies the head field for the tracer migration calculations. The heads are solved in a 4-level multigrid program.

4. Borehole tests are simulated with a transient model. For the sake of computer run times, the transient hydraulic tests are performed in a grid twice as coarse (337x257). This appeared to give only minor differences from the finer grid results. Transient responses are limited to about 100 seconds of simulated time. Cross-hole tests are available at boreholes near the opened borehole. We expect to have longer-term transient tests available in the near future.

E. Sampling strategy - The location of boreholes, shafts and tunnels correspond as nearly as possible to the actual locations in the Grimsel Rock Laboratory. At the request of a participant, additional boreholes and tests will be performed within reasonable limits of (real-world) expected cost and feasibility, and computational resources of the pilot team.

F. Independence between data sets - Not applicable

G. Biases Inherent in the Design - Since this is a simulated geosphere, there is an inherent danger of introducing our bias to the model, therefore making it unrealistic. These concerns are addressed by specifying the rules that apply to the synthetic geospheres as discussed in Section I.F.

Tracer experiments initially will be for non-sorbing, non-diffusing tracer particles. Matrix diffusion and sorption will be studied in Phase II of this exercise.

## III. CURRENT STATUS AND EXPERIMENTAL SCHEDULE

The Phase I modeling is complete, except for additional requests that might be made by the participating modelers. The results are presented in the Appendix. The authors will present a "modeler's" interpretation of the experimental results at the Helsinki meeting, and predict the breakthrough to open boreholes and the experimental drift of tracer introduced at low pressure to one of the peripheral boreholes.

Models to include diffusion and geochemical retardation are being developed for Phase II of this experiment.

Parts of the synthetic experiments are being duplicated by separate teams from NRC and NAGRA in order to confirm that the models for calculating the synthetic data are correct and free from computational problems. Present transient tests are limited to about 100 seconds, and are only applicable to nearby boreholes.

## IV. EXPERIMENTAL RESULTS

Geometrical information for setting up the problem was distributed at the Tucson meeting, Nov.14-18, 1988.

The following data has been included in the Appendix:

A. Raw Data - configuration of mountainside, head and outflow in boreholes and tunnels, response to pressure tests in boreholes, increases in flow rate to tunnels from borehole pressure disturbances, breakthrough curves for simulated dipole tracer tests, and arrival of tracer at the experimental drift.

B. Processed data - Interpretation of the raw data is left to the the modeler.

C. Data Storage - All data from the simulated tests are available in printed form, floppy disks and on BITNET.

## V. PREVIOUS MODELING

Codell (1988) presented a two dimensional synthetic migration experiment on a repository-scale problem (about 10 kilometer scale), in which he tested the ability to predict the performance of the repository on the basis of limited samples. Cole (1987) has performed numerical laboratory experiments of the movement of tracers on both small scale heterogeneous soils and large scale regional models. The Grimsel site itself has been digitized for modeling exercises (Herzog, 1988), but not in connection with a synthetic data set, nor at the overall fine resolution of this experiment.

## VI EXPECTATION FROM INTRAVAL PARTICIPATION

A. Experimentalists' View - The experimenters will be those individuals who will run the computer models composing the synthetic geosphere. They will simulate tests, and will work with the modelers to interpret them. On the basis of this interpretation, both the experimentalists and the modelers will specify the locations and types of additional tests.

The experimentalists will benefit from comparing interpretations of the parameters and their distribution to the synthetic geosphere and understanding how possible misinterpretations had occurred. In addition, the experimentalists could gain insight into which types of tests provide the best data in terms of the ultimate goal of the predictive model; e.g., transport of tracer.

B. Modelers' View - The modeler will be presented with the results of a limited number of tests on the synthetic geosphere, and will be asked to estimate the performance measure on the basis of these limited data. The performance measure will be the breakthrough at open boreholes and the experimental drift of tracer released at very low injection rates in peripheral boreholes and moving under the steady-state, non-uniform gradient. Details of the performance tests

are given in the appendix. The results of the modeler's prediction will be compared to the "true" breakthrough calculated from the detailed synthetic geosphere model. The worth of various modeling and characterization strategies can therefore be determined. The modeler will work closely with the experimentalists to plan the collection of additional data to refine the predictive models.

## VII INFORMATION EXCHANGE

### Addresses of Key Personnel

Richard Codell
U.S. Nuclear Regulatory Commission
Washington D.C. 20555
Phone (301)-492-0408
BITNET address: VZZ@NIHCU

Stratis Vomvoris
NAGRA
Parkstrasse 23
Baden Switzerland
Phone: 056/205 324
BITNET address: JTROESCH@CZHETH5A, subject STRATIS VOMVORIS

Charles Cole
Pacific Northwest Labs
Post Office Box 999
Richland Washington 99352
Phone: (509) 376-8451

## VIII POSSIBILITIES FOR FUTURE EXPERIMENTS AND DATA COLLECTION

The pilot team is working on an improved transient model for simulating borehole hydraulic tests for longer periods of time, and will provide these results at the earliest opportunity.

Synthetic geosphere models are being developed to take into account the complications of matrix diffusion and geochemical sorption, discrete fractures and other discontinuities in the heterogeneous but continuous medium, and geochemical sorption. These will be presented in Phase II of this exercise.

Additional synthetic sites could be created, possibly based on actual INTRAVAL cases. These would be useful for investigating the range of interpretations of the real-world site's data.

## IX OUTPUT FORMAT

Output for the prediction of tracer migration experiments should be in the form of tracer breakthrough curves, with estimates of uncertainty.

## X REFERENCES


Codell, R., "Testing site characterization strategies with synthetic data bases", Presented at "Hydrogeologic Aspects of Radioactive Waste Disposal", Geological Society of America, Portland Maine, March 12, 1988

Cole, C. and Foote, H., "Use of multigrid techniques to study effects of limited sampling of heterogeneity on transport predictions", National Water Well Association Conference, Denver Colorado, February 10-12, 1987

Hadermann, J., Private communication, 1988.

Herzog, F., "Hydraulisches Modell fur die Migrationszone im Felslabor Grimsel", PSI-TM-431-88-04, Paul Scherrer Institut, July 1988.

Hewitt, "Fractal distributions of reservoir heterogeneity and their influence on fluid transport", SPE 15386, Society of Petroleum Engineers, October 1986

Hufschmied, P., J.Hadermann, F. Herzog, "Proposal for a synthetic migration experiment with the purpose of studying validation strategies for geosphere performance models", INTRAVAL ad hoc group meeting, April 17-18, Stockholm

Jeffery, T., "Mimicking mountains", BYTE, December, 1987

Winkler,K, J.Chalmers, S.Hodson, P.Woodward, and N.Zabusky, "A Numerical Laboratory", Physics Today, October, 1987

Appendix A, INTRAVAL Problem 6
Synthetic Migration Experiment
Data Sets

## A.1. Introduction

The "data" presented here represent the results of simulated measurements on the INTRAVAL Problem 6 synthetic geosphere, which is patterned after the real-world migration experiment at the Grimsel Rock Laboratory. There are three types of data:

1. Steady-state hydraulic test data consisting of head and flow measurements at boreholes and tunnels.

2. Transient hydraulic test data consisting of head and flow measurements in boreholes as a result of opening one borehole to the head in the center of the experimental drift. We have provided a floppy disk with all of the transient data in ASCII format.

3. Breakthrough data consisting of the arrival time distribution of tracer (represented as diffusionless particles) released instantaneously in a dipole experiment. Where applicable, the arrival at locations other than the extraction well (i.e., the experimental drift) has also been given.

The datum for all hydraulic tests is the center of the experimental drift, where the head is specified to be zero.

## A.2 Steady-state hydraulic test data

Table A1 gives the results of steady state measurements of head and flow in the boreholes and tunnels of the site. It consists of steady-state head for all boreholes closed, steady state head for opening one or two boreholes at a time, outflow or inflow to the boreholes when opened, and outflow at the tunnels.

## A.3 Transient hydraulic test data

Table A2 gives the results of the transient borehole tests. For each test, a borehole is opened, setting its head to zero. The outflow or inflow of water from the open borehole and the pressure response in several nearby closed boreholes are presented as a function of time. Note that all boreholes except borehole 10 have outflow from the open boreholes and drawdown in the closed boreholes (i.e., negative sign for Q and S). Water would flow into rather than out of borehole 10. Table A2(i) for borehole 11 presents only outflow and not drawdown for surrounding boreholes. For convenience, An ASCII version of Tables A1 and A2 has been created on a floppy disk and a BITNET file for distribution. The project team will distribute the disk at the Helsinki meeting.

A4. Breakthrough data

Figures A1 and A2 present the cumulative arrival time distribution for diffusionless inert tracer introduced instantaneously at two dipole tests. The first test is between boreholes 4 and 6, with 0.2 liters per minute injected to borehole 4 and 0.4 liters per minute extracted from borehole 6. Recovery of tracer is 100%. The second test is between boreholes 9 and 7, with injection of 0.2 liters per minute in borehole 9 and extraction of 0.4 liters per minute at borehole 7. Recovery in borehole 7 is 47.5%, with the rest of the tracer arriving at the experimental drift. The breakthrough curve for tracer arrival at the experimental drift is also given on Figure A2.*

A5. Performance Measure Tests

The model validation will be on the basis of breakthrough curves at open boreholes and the experimental drift for tracer introduced at boreholes 4, 5 and 11 (only one borehole at a time). Tracer will be introduced instantaneously with a flowrate at the injection boreholes of 0.05 liters per minute. Collection boreholes will be 6, 7, 8 and 9. Flows at the collection boreholes will be limited to 0.1 liters per minute or the normal outflow, whichever is less. Borehole 10 will be closed. Injection at boreholes 4, 5 and 11 will be 0.05 liters per minute, regardless of whether there is tracer injection or not (this is primarily for convenience, permitting us to perform all of the tracer experiments with only one calculation of the flow field. We do not expect that the small injection rates would have a significant effect on the flow field for the purposes of this test).

Results for release of tracer from borehole 4 and collection at boreholes 6, 7, 8, 9 and the experimental drift will be presented at the Helsinki meeting along with an attempted model validation.

*Collection of simulated tracer poses no special problems in the numerical experiments, but would be difficult in practice in the real experimental drift. Planned experiments at Grimsel would rely mainly on collection of tracer at boreholes.

Table A1(a)
Steady State Hydraulic Head Results, meters
relative to center of experimental drift

| Borehole and location* | closed | open 4&5 | open 6&7 | open 8&9 | open 10 |
|---|---|---|---|---|---|
| 4(-10.3,-6.0) | 6.105 | 0 | 5.498 | 5.757 | 6.093 |
| 5(5.8,-3.65) | 0.8 | 0 | 0.756 | 0.772 | 0.875 |
| 6(-4.6,-5.3) | 2.953 | 2.592 | 0 | 2.325 | 2.94 |
| 7(-6.05,-3.5) | 3.736 | 3.427 | 0 | 3.452 | 3.727 |
| 8(-1.5,-4.5) | 0.494 | 0.388 | -0.029 | 0 | 0.506 |
| 9(-6,-7.5) | 3.814 | 3.092 | 2.38 | 0 | 3.8 |
| 10(3,-2.7) | -0.31 | -0.392 | -0.351 | -0.334 | 0 |
| 11(-15.3,4) | 8.915 | 8.89 | 8.89 | 8.907 | 8.912 |

*meters, relative to center of experimental drift, positive direction is up.

Table A1(b)

Steady-state flow rate into experimental drift, cubic meters/second in response to opening boreholes (positive means flow into the drift)

| closed | open 4&5 | open 6&7 | open 8&9 | open10 |
|---|---|---|---|---|
| 3.877E-5 | 3.808E-5 | 3.662E-5 | 3.826E-5 | 3.889E-5 |

Table A1(c)
Steady-state flows from open boreholes, cubic meters/second
(negative means flow out)

| Borehole | open 4&5 | open 6&7 | open 8&9 | open 10 |
|---|---|---|---|---|
| 4 | -2.94E-6 | | | |
| 5 | -2.52E-7 | | | |
| 6 | | -1.64E-6 | | |
| 7 | | -3.78E-6 | | |
| 8 | | | -1.86E-7 | |
| 9 | | | -1.32E-6 | |
| 10 | | | | +2.25E-7 |

Table A1(d) - Miscellaneous Flowrates from other Tunnels with all boreholes closed

Tunnel 5 = 4.055E-5 cubic meters/second out

Tunnel 7 = 4.79E-6 cubic meters/second out

Tunnel 8 = 3.7E-6 cubic meters/second out

Table A2(a) Flowrate Q in borehole 4 and drawdown S in boreholes 6, 7 and 9 from opening borehole 4 to zero head

| time, sec | Q, cu m/s | S - 6, m | S - 7, m | S - 9, m |
|---|---|---|---|---|
| 0.440 | -5.53E-06 | 0.000 | 0.000 | 0.000 |
| 0.728 | -4.97E-06 | 0.000 | 0.000 | 0.000 |
| 1.070 | -4.64E-06 | 0.000 | 0.000 | 0.000 |
| 1.490 | -4.41E-06 | 0.000 | -0.001 | 0.000 |
| 1.990 | -4.23E-06 | 0.000 | -0.002 | 0.000 |
| 2.580 | -4.08E-06 | -0.001 | -0.005 | -0.001 |
| 3.300 | -3.95E-06 | -0.002 | -0.010 | -0.004 |
| 4.160 | -3.83E-06 | -0.004 | -0.017 | -0.008 |
| 5.190 | -3.73E-06 | -0.008 | -0.028 | -0.016 |
| 6.430 | -3.64E-06 | -0.014 | -0.042 | -0.028 |
| 7.920 | -3.56E-06 | -0.023 | -0.059 | -0.046 |
| 9.700 | -3.48E-06 | -0.036 | -0.079 | -0.070 |
| 11.800 | -3.41E-06 | -0.053 | -0.100 | -0.101 |
| 14.400 | -3.35E-06 | -0.074 | -0.123 | -0.139 |
| 17.500 | -3.29E-06 | -0.098 | -0.146 | -0.182 |
| 21.200 | -3.24E-06 | -0.125 | -0.170 | -0.231 |
| 25.600 | -3.20E-06 | -0.155 | -0.194 | -0.284 |
| 30.900 | -3.16E-06 | -0.186 | -0.217 | -0.340 |
| 37.300 | -3.13E-06 | -0.218 | -0.240 | -0.397 |
| 45.000 | -3.10E-06 | -0.250 | -0.261 | -0.455 |
| 54.200 | -3.07E-06 | -0.282 | -0.282 | -0.512 |
| 65.200 | -3.05E-06 | -0.312 | -0.302 | -0.566 |
| 78.500 | -3.03E-06 | -0.340 | -0.320 | -0.618 |
| 94.400 | -3.01E-06 | -0.366 | -0.337 | -0.666 |

Table A2(b) Flowrate Q in borehole 5 and drawdown S in boreholes 8 and 10 from opening borehole 5 to zero head

| time, sec | Q cu m/s | S - 8, m | S - 10, m |
|---|---|---|---|
| 0.200 | -8.33E-07 | 0.000 | 0.000 |
| 0.440 | -6.16E-07 | 0.000 | 0.000 |
| 0.728 | -5.42E-07 | 0.000 | 0.000 |
| 1.070 | -4.98E-07 | 0.000 | 0.000 |
| 1.490 | -4.67E-07 | 0.000 | -0.001 |
| 1.990 | -4.42E-07 | 0.000 | -0.002 |
| 2.580 | -4.22E-07 | 0.000 | -0.004 |
| 3.300 | -4.04E-07 | 0.000 | -0.006 |
| 4.160 | -3.88E-07 | 0.000 | -0.010 |
| 5.190 | -3.74E-07 | 0.000 | -0.014 |
| 6.430 | -3.62E-07 | 0.000 | -0.019 |
| 7.920 | -3.50E-07 | 0.000 | -0.024 |
| 9.700 | -3.39E-07 | 0.000 | -0.029 |
| 11.800 | -3.30E-07 | 0.000 | -0.035 |
| 14.400 | -3.21E-07 | -0.001 | -0.040 |
| 17.500 | -3.12E-07 | -0.001 | -0.045 |
| 21.200 | -3.05E-07 | -0.001 | -0.050 |
| 25.600 | -2.98E-07 | -0.002 | -0.055 |
| 30.900 | -2.91E-07 | -0.002 | -0.059 |
| 37.300 | -2.86E-07 | -0.003 | -0.062 |
| 45.000 | -2.80E-07 | -0.004 | -0.065 |
| 54.200 | -2.76E-07 | -0.005 | -0.068 |
| 65.200 | -2.72E-07 | -0.005 | -0.070 |
| 78.500 | -2.68E-07 | -0.006 | -0.073 |
| 94.400 | -2.65E-07 | -0.007 | -0.074 |

Table A2(c) Flowrate Q in borehole 6 and drawdown S in boreholes 7, 8 and 9 from opening borehole 6 to zero head

| time, sec | Q - 6, m/s | S - 7, m | S - 8, m | S - 9, m |
|---|---|---|---|---|
| 0.440 | -4.21E-06 | -0.005 | -0.000 | -0.001 |
| 0.728 | -3.81E-06 | -0.018 | -0.001 | -0.004 |
| 1.070 | -3.55E-06 | -0.038 | -0.002 | -0.011 |
| 1.490 | -3.37E-06 | -0.065 | -0.006 | -0.024 |
| 1.990 | -3.22E-06 | -0.096 | -0.014 | -0.045 |
| 2.580 | -3.09E-06 | -0.130 | -0.025 | -0.074 |
| 3.300 | -2.97E-06 | -0.166 | -0.042 | -0.111 |
| 4.160 | -2.87E-06 | -0.201 | -0.063 | -0.155 |
| 5.190 | -2.79E-06 | -0.235 | -0.087 | -0.205 |
| 6.430 | -2.71E-06 | -0.267 | -0.115 | -0.259 |
| 7.920 | -2.64E-06 | -0.296 | -0.144 | -0.318 |
| 9.700 | -2.57E-06 | -0.324 | -0.173 | -0.379 |
| 11.800 | -2.52E-06 | -0.349 | -0.202 | -0.440 |
| 14.400 | -2.47E-06 | -0.372 | -0.229 | -0.502 |
| 17.500 | -2.43E-06 | -0.392 | -0.253 | -0.563 |
| 21.200 | -2.39E-06 | -0.410 | -0.274 | -0.622 |
| 25.600 | -2.36E-06 | -0.427 | -0.293 | -0.677 |
| 30.900 | -2.33E-06 | -0.441 | -0.309 | -0.729 |
| 37.300 | -2.31E-06 | -0.454 | -0.323 | -0.777 |
| 45.000 | -2.29E-06 | -0.465 | -0.335 | -0.821 |
| 54.200 | -2.27E-06 | -0.475 | -0.345 | -0.860 |
| 65.200 | -2.25E-06 | -0.484 | -0.354 | -0.895 |
| 78.500 | -2.24E-06 | -0.492 | -0.363 | -0.926 |
| 94.400 | -2.23E-06 | -0.499 | -0.370 | -0.953 |

Table A2(d) Flowrate Q from borehole 7 and drawdown S in boreholes 4, 6, 8 and 9 from opening borehole 7 to zero head.

| time,sec | Q - 7, cu m/s | S - 4, m | S - 6, m | S - 8, m | S - 9, m |
|---|---|---|---|---|---|
| 0.224 | -6.47E-06 | 0 | 0 | 0 | 0 |
| 0.272 | -6.30E-06 | 0 | -0.001 | 0 | 0 |
| 0.328 | -6.14E-06 | 0 | -0.002 | 0 | 0 |
| 0.394 | -6.00E-06 | 0 | -0.004 | 0 | 0 |
| 0.471 | -5.88E-06 | 0 | -0.007 | 0 | 0 |
| 0.561 | -5.76E-06 | 0 | -0.012 | 0 | 0 |
| 0.666 | -5.65E-06 | 0 | -0.02 | 0 | 0 |
| 0.79 | -5.55E-06 | 0 | -0.03 | 0 | 0 |
| 0.934 | -5.46E-06 | 0 | -0.044 | 0 | 0 |
| 1.1 | -5.37E-06 | 0 | -0.062 | 0 | -0.001 |
| 1.3 | -5.29E-06 | -0.001 | -0.083 | -0.001 | -0.002 |
| 1.53 | -5.22E-06 | -0.001 | -0.109 | -0.001 | -0.003 |
| 1.8 | -5.15E-06 | -0.002 | -0.138 | -0.002 | -0.006 |
| 2.12 | -5.08E-06 | -0.004 | -0.17 | -0.004 | -0.01 |
| 2.49 | -5.02E-06 | -0.008 | -0.206 | -0.007 | -0.017 |
| 2.92 | -4.96E-06 | -0.013 | -0.244 | -0.012 | -0.026 |
| 3.43 | -4.90E-06 | -0.02 | -0.284 | -0.018 | -0.039 |
| 4.02 | -4.84E-06 | -0.029 | -0.326 | -0.026 | -0.056 |
| 4.71 | -4.79E-06 | -0.041 | -0.369 | -0.036 | -0.077 |
| 5.53 | -4.74E-06 | -0.055 | -0.412 | -0.048 | -0.102 |
| 6.47 | -4.70E-06 | -0.073 | -0.456 | -0.061 | -0.132 |
| 7.59 | -4.65E-06 | -0.093 | -0.5 | -0.076 | -0.165 |
| 8.88 | -4.61E-06 | -0.115 | -0.542 | -0.092 | -0.203 |
| 10.4 | -4.57E-06 | -0.14 | -0.584 | -0.108 | -0.243 |
| 12.2 | -4.54E-06 | -0.166 | -0.624 | -0.125 | -0.287 |
| 14.3 | -4.50E-06 | -0.194 | -0.662 | -0.141 | -0.332 |
| 16.7 | -4.47E-06 | -0.223 | -0.697 | -0.157 | -0.378 |
| 19.5 | -4.44E-06 | -0.253 | -0.731 | -0.173 | -0.425 |
| 22.9 | -4.42E-06 | -0.283 | -0.762 | -0.188 | -0.471 |
| 26.8 | -4.39E-06 | -0.313 | -0.791 | -0.202 | -0.517 |
| 31.3 | -4.37E-06 | -0.343 | -0.817 | -0.215 | -0.561 |
| 36.7 | -4.35E-06 | -0.372 | -0.841 | -0.227 | -0.604 |
| 42.9 | -4.33E-06 | -0.401 | -0.863 | -0.238 | -0.644 |
| 50.2 | -4.31E-06 | -0.43 | -0.883 | -0.248 | -0.682 |
| 58.8 | -4.29E-06 | -0.457 | -0.901 | -0.257 | -0.717 |
| 68.8 | -4.27E-06 | -0.485 | -0.917 | -0.266 | -0.75 |
| 80.5 | -4.26E-06 | -0.511 | -0.932 | -0.274 | -0.78 |
| 94.2 | -4.24E-06 | -0.537 | -0.947 | -0.282 | -0.808 |

Table A2(e) Flowrate Q in borehole 8 and drawdown S in boreholes 6, 7 and 8 from opening borehole 8 to zero head

| time,sec | Q - 8, cu m/s | S - 6, m | S - 7, m | S - 9, m |
|---|---|---|---|---|
| 0.44 | -4.50E-07 | 0.000 | 0.000 | 0.000 |
| 0.728 | -4.06E-07 | 0.000 | 0.000 | 0.000 |
| 1.07 | -3.81E-07 | 0.000 | 0.000 | 0.000 |
| 1.49 | -3.63E-07 | -0.001 | 0.000 | 0.000 |
| 1.99 | -3.49E-07 | -0.002 | 0.000 | 0.000 |
| 2.58 | -3.38E-07 | -0.003 | 0.000 | 0.000 |
| 3.3 | -3.29E-07 | -0.005 | -0.001 | 0.000 |
| 4.16 | -3.21E-07 | -0.007 | -0.002 | 0.000 |
| 5.19 | -3.14E-07 | -0.010 | -0.002 | -0.001 |
| 6.43 | -3.09E-07 | -0.013 | -0.003 | -0.001 |
| 7.92 | -3.04E-07 | -0.017 | -0.005 | -0.002 |
| 9.7 | -3.00E-07 | -0.020 | -0.006 | -0.003 |
| 11.8 | -2.97E-07 | -0.024 | -0.007 | -0.004 |
| 14.4 | -2.95E-07 | -0.027 | -0.009 | -0.006 |
| 17.5 | -2.93E-07 | -0.030 | -0.010 | -0.008 |
| 21.2 | -2.91E-07 | -0.033 | -0.012 | -0.011 |
| 25.6 | -2.89E-07 | -0.036 | -0.013 | -0.013 |
| 30.9 | -2.88E-07 | -0.039 | -0.014 | -0.016 |
| 37.3 | -2.87E-07 | -0.041 | -0.015 | -0.019 |
| 45 | -2.86E-07 | -0.043 | -0.016 | -0.022 |
| 54.2 | -2.85E-07 | -0.045 | -0.017 | -0.025 |
| 65.2 | -2.84E-07 | -0.046 | -0.018 | -0.028 |
| 78.5 | -2.83E-07 | -0.048 | -0.019 | -0.030 |
| 94.4 | -2.83E-07 | -0.049 | -0.020 | -0.033 |

Table A2(g) Flowrate Q from borehole 9 and drawdown S in boreholes 4, 6 and 7 resulting from opening borehole 9 to zero head

| time,sec | Q - 9, cu m/s | S - 4, m | S - 6, m | S - 7, m |
|---|---|---|---|---|
| 0.440 | -3.01E-06 | 0.000 | -0.001 | 0.000 |
| 0.728 | -2.67E-06 | 0.000 | -0.003 | 0.000 |
| 1.070 | -2.48E-06 | 0.000 | -0.007 | 0.000 |
| 1.490 | -2.34E-06 | 0.000 | -0.016 | -0.001 |
| 1.990 | -2.22E-06 | 0.000 | -0.030 | -0.003 |
| 2.580 | -2.13E-06 | -0.001 | -0.049 | -0.007 |
| 3.300 | -2.05E-06 | -0.002 | -0.074 | -0.013 |
| 4.160 | -1.98E-06 | -0.004 | -0.103 | -0.021 |
| 5.190 | -1.91E-06 | -0.008 | -0.136 | -0.032 |
| 6.430 | -1.85E-06 | -0.015 | -0.172 | -0.046 |
| 7.920 | -1.79E-06 | -0.023 | -0.210 | -0.062 |
| 9.700 | -1.74E-06 | -0.036 | -0.250 | -0.079 |
| 11.800 | -1.70E-06 | -0.051 | -0.291 | -0.098 |
| 14.400 | -1.65E-06 | -0.069 | -0.332 | -0.118 |
| 17.500 | -1.61E-06 | -0.090 | -0.372 | -0.137 |
| 21.200 | -1.57E-06 | -0.113 | -0.410 | -0.157 |
| 25.600 | -1.54E-06 | -0.138 | -0.445 | -0.175 |
| 30.900 | -1.51E-06 | -0.164 | -0.478 | -0.193 |
| 37.300 | -1.48E-06 | -0.191 | -0.508 | -0.209 |
| 45.000 | -1.46E-06 | -0.217 | -0.534 | -0.223 |
| 54.200 | -1.43E-06 | -0.243 | -0.557 | -0.237 |
| 65.200 | -1.41E-06 | -0.267 | -0.576 | -0.248 |
| 78.500 | -1.40E-06 | -0.289 | -0.592 | -0.258 |
| 94.400 | -1.38E-06 | -0.310 | -0.604 | -0.267 |

Table A2(h) Flowrate Q from borehole 10 and drawdowns in boreholes 5 and 8 resulting from opening borehole 10 to zero head. Note: flow is into rather than discharging from borehole 10 and drawdowns are positive pressures.

| time, sec | Q - cu m/s | S - 5, m | S - 8, m |
|---|---|---|---|
| 0.200 | 4.54E-07 | 0.000 | 0.000 |
| 0.440 | 3.54E-07 | 0.000 | 0.000 |
| 0.728 | 3.22E-07 | 0.000 | 0.000 |
| 1.070 | 3.03E-07 | 0.000 | 0.000 |
| 1.490 | 2.90E-07 | 0.001 | 0.000 |
| 1.990 | 2.80E-07 | 0.001 | 0.000 |
| 2.580 | 2.72E-07 | 0.002 | 0.000 |
| 3.300 | 2.66E-07 | 0.004 | 0.000 |
| 4.160 | 2.61E-07 | 0.006 | 0.001 |
| 5.190 | 2.57E-07 | 0.009 | 0.001 |
| 6.430 | 2.53E-07 | 0.012 | 0.002 |
| 7.920 | 2.50E-07 | 0.016 | 0.002 |
| 9.700 | 2.48E-07 | 0.020 | 0.003 |
| 11.800 | 2.46E-07 | 0.024 | 0.003 |
| 14.400 | 2.44E-07 | 0.028 | 0.004 |
| 17.500 | 2.42E-07 | 0.032 | 0.005 |
| 21.200 | 2.41E-07 | 0.036 | 0.005 |
| 25.600 | 2.40E-07 | 0.040 | 0.006 |
| 30.900 | 2.39E-07 | 0.044 | 0.006 |
| 37.300 | 2.38E-07 | 0.048 | 0.007 |
| 45.000 | 2.37E-07 | 0.051 | 0.007 |
| 54.200 | 2.36E-07 | 0.055 | 0.008 |
| 65.200 | 2.35E-07 | 0.058 | 0.008 |
| 78.500 | 2.35E-07 | 0.060 | 0.008 |
| 94.400 | 2.34E-07 | 0.063 | 0.009 |

Table A2(i) Flowrate Q from borehole 11 in response to opening it to zero head

| time - sec | Q -11, cu m/s |
|---|---|
| 0.44 | -9.61E-05 |
| 0.728 | -8.72E-05 |
| 1.07 | -8.10E-05 |
| 1.49 | -7.58E-05 |
| 1.99 | -7.12E-05 |
| 2.58 | -6.68E-05 |
| 3.3 | -6.26E-05 |
| 4.16 | -5.86E-05 |
| 5.19 | -5.48E-05 |
| 6.43 | -5.11E-05 |
| 7.92 | -4.75E-05 |
| 9.7 | -4.40E-05 |
| 11.8 | -4.05E-05 |
| 14.4 | -3.72E-05 |
| 17.5 | -3.39E-05 |
| 21.2 | -3.07E-05 |
| 25.6 | -2.77E-05 |
| 30.9 | -2.48E-05 |
| 37.3 | -2.20E-05 |
| 45 | -1.94E-05 |
| 54.2 | -1.69E-05 |
| 65.2 | -1.46E-05 |
| 78.5 | -1.25E-05 |
| 94.4 | -1.05E-05 |
| 113 | -8.78E-06 |
| 136 | -7.24E-06 |

Figure 1

# Measureability of Test Sites

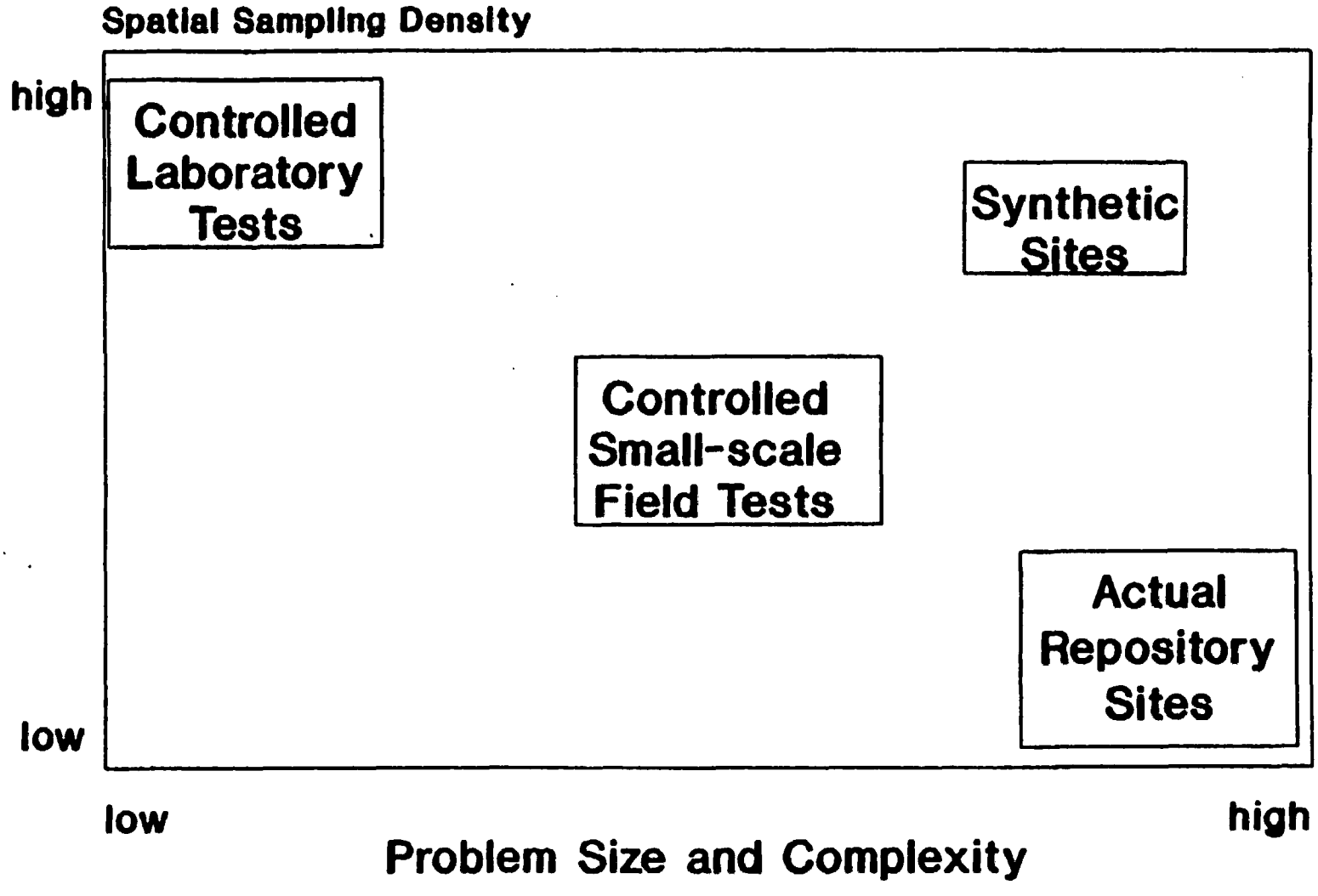

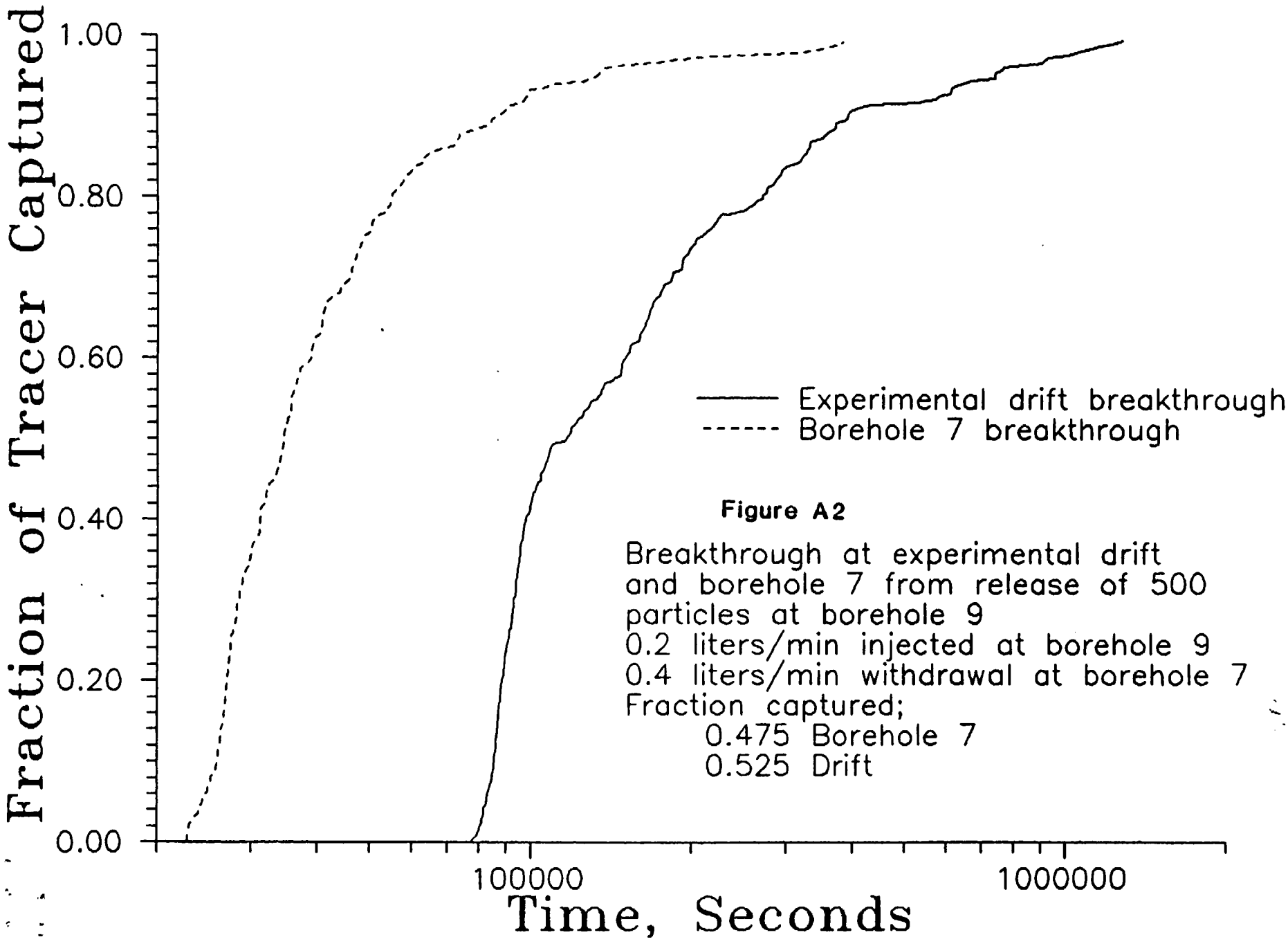


**Figure A2**

Breakthrough at experimental drift and borehole 7 from release of 500 particles at borehole 9
0.2 liters/min injected at borehole 9
0.4 liters/min withdrawal at borehole 7
Fraction captured;
0.475 Borehole 7
0.525 Drift

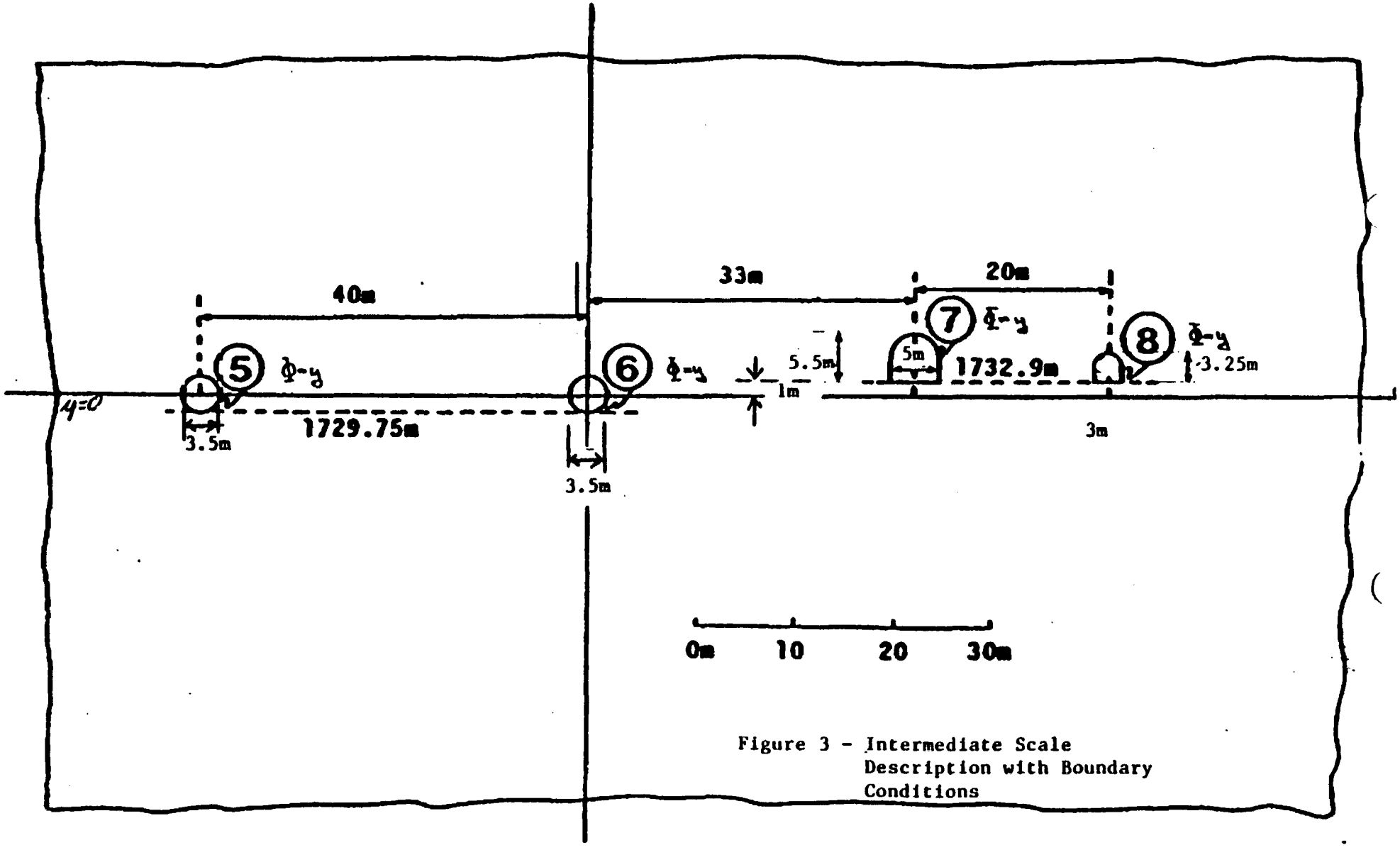


Figure 3 - Intermediate Scale Description with Boundary Conditions

Corrected 6/9/89

Note: Previous Figure A1 was in error

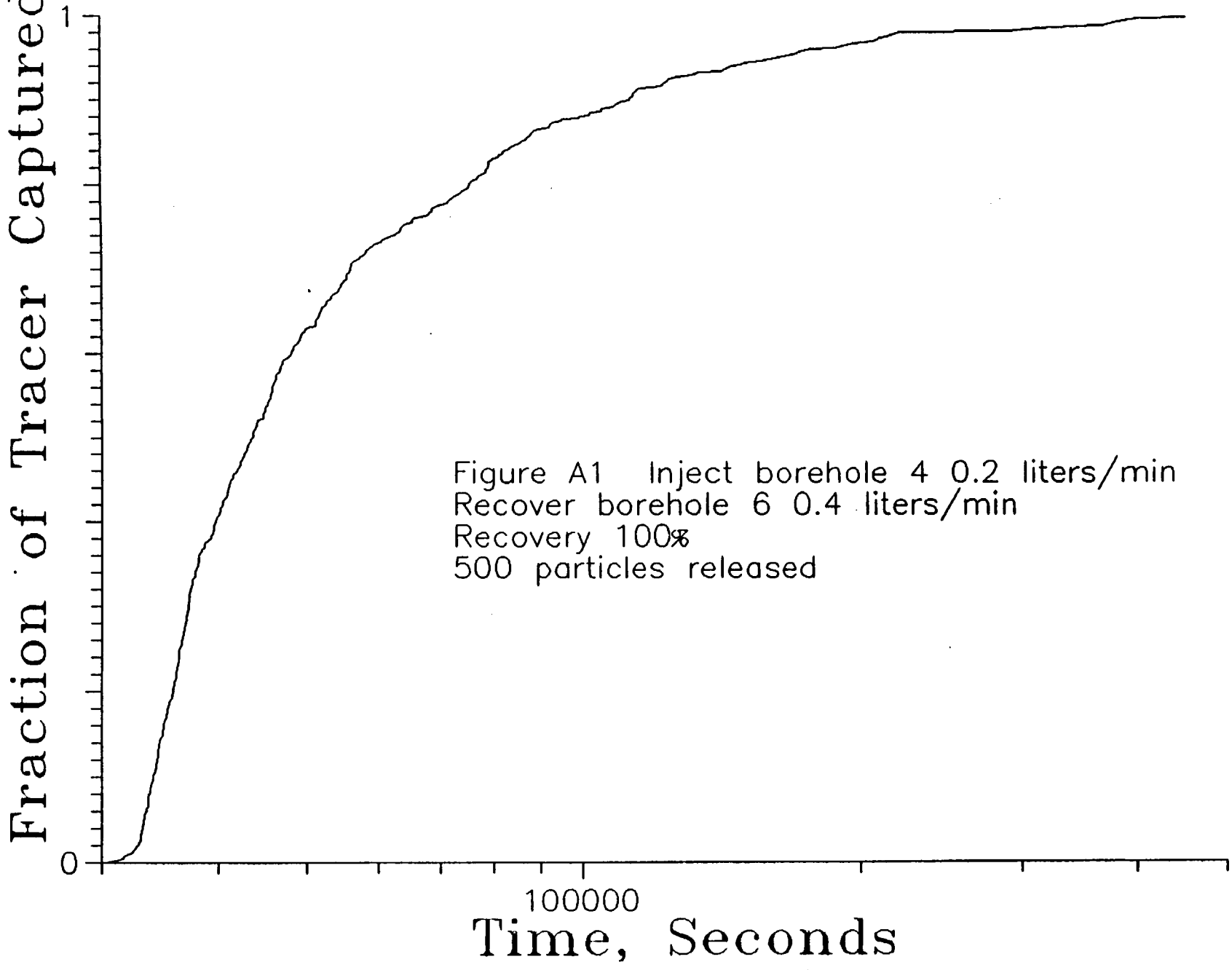


Figure A1 Inject borehole 4 0.2 liters/min
Recover borehole 6 0.4 liters/min
Recovery 100%
500 particles released

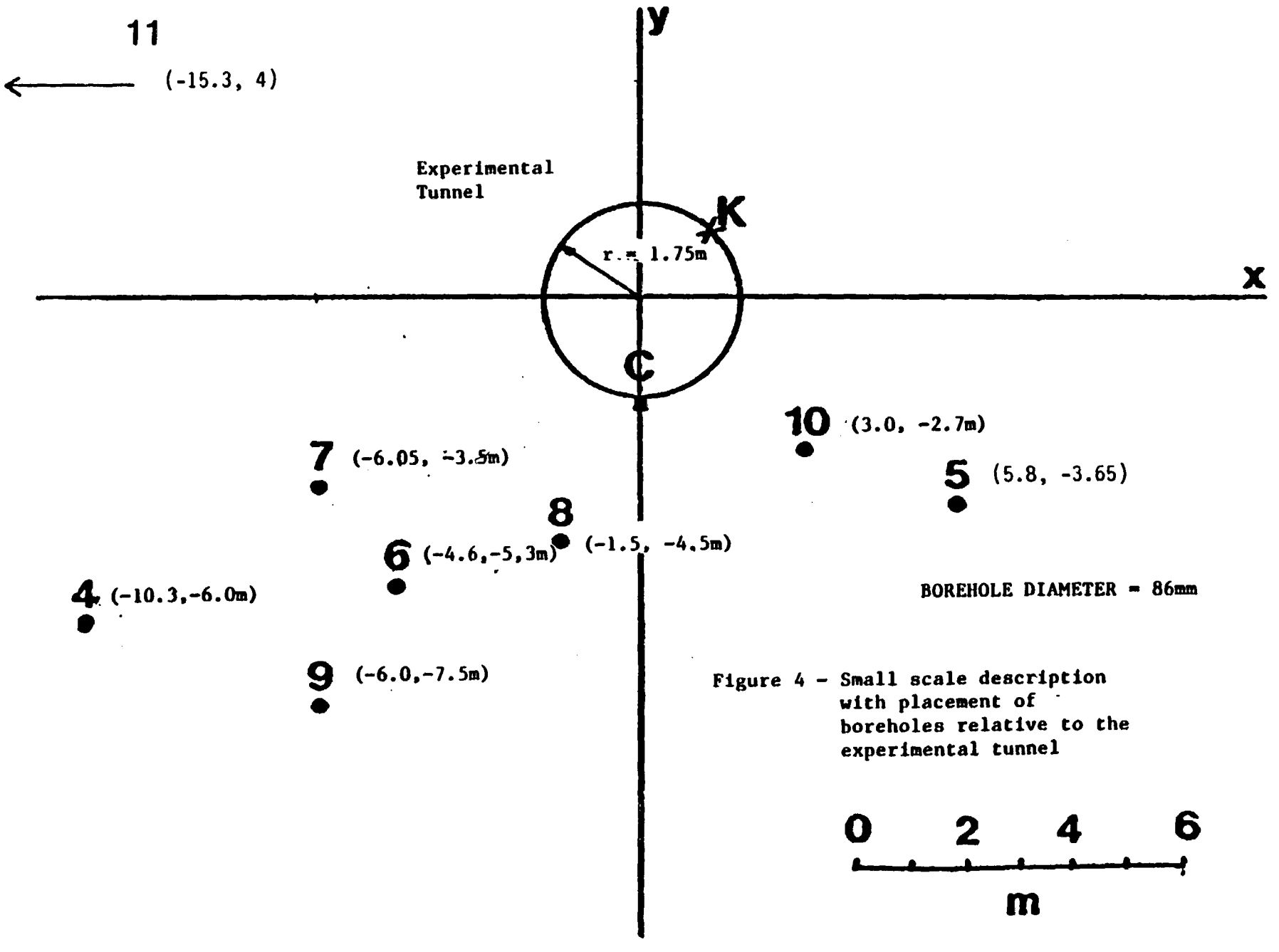


Figure 4 - Small scale description with placement of boreholes relative to the experimental tunnel

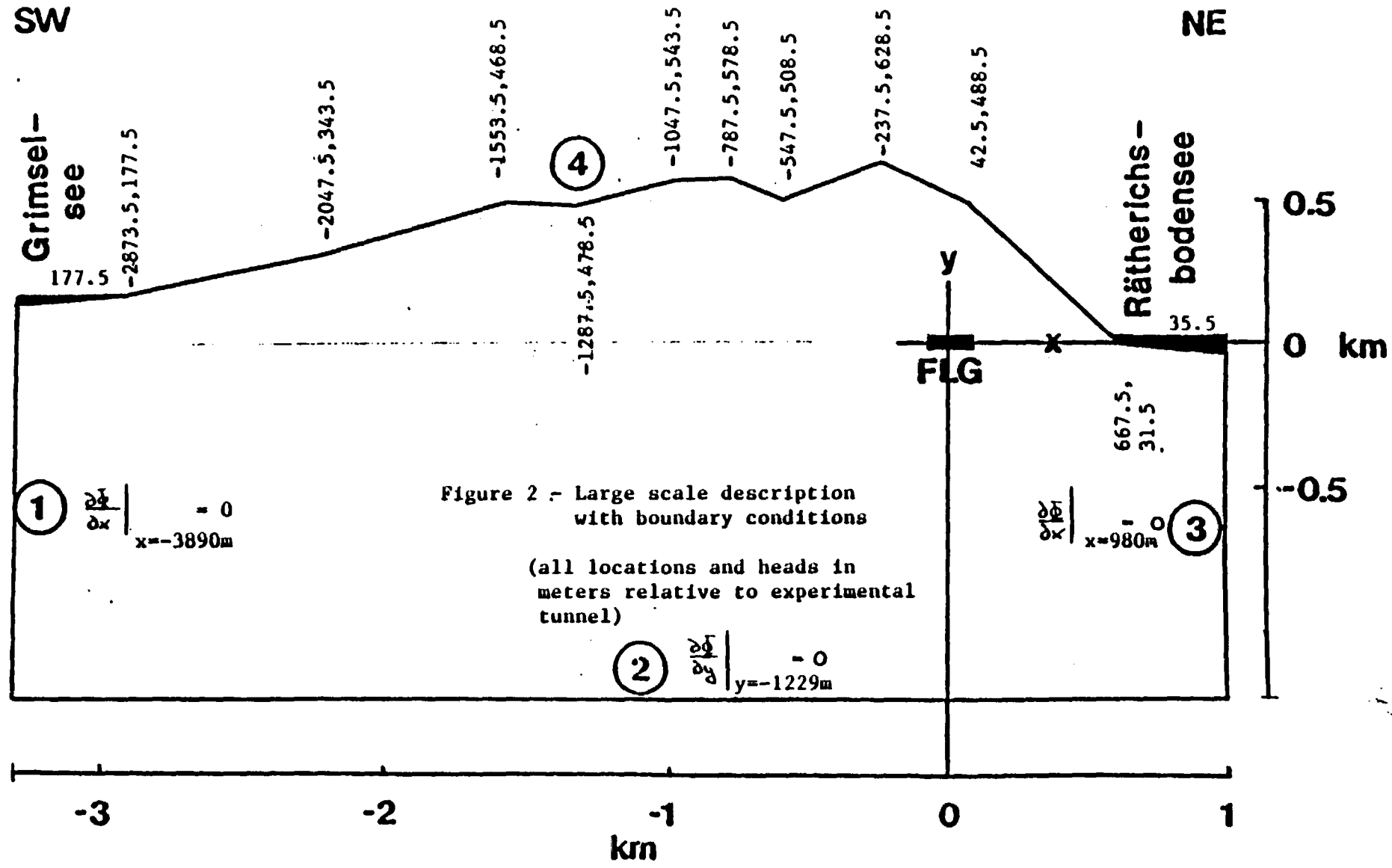


Figure 2 - Large scale description with boundary conditions

(all locations and heads in meters relative to experimental tunnel)